Strong temperature-dependent-viscosity effects on a rivulet draining down a uniformly heated or cooled slowly varying substrate

S. K. Wilson[1] and B. R. Duffy

Department of Mathematics,
University of Strathclyde,
Livingstone Tower,
26 Richmond Street,
Glasgow G1 1XH,
United Kingdom

Running Title : Temperature-dependent-viscosity effects on a rivulet

1st February 2002, revised 2nd August and 4th December 2002

Abstract

We use the lubrication approximation to investigate the steady locally unidirectional gravity-driven draining of a thin rivulet of Newtonian fluid with temperature-dependent viscosity down a slowly varying substrate that is either uniformly hotter or uniformly colder than the surrounding atmosphere. We consider the situation in which the Biot number (and hence the variation of temperature across the rivulet) is small, but in which the variation of viscosity with temperature is sufficiently strong that thermoviscosity effects appear at leading order in the limit of small Biot number. Three different models for the dependence of viscosity on temperature (specifically, the linear, exponential and Eyring models) are considered, but our attention is concentrated on the more realistic exponential and Eyring models (which coincide

[1]Author for correspondence. Telephone : + 44 (0)141 548 3820, Fax : + 44 (0)141 552 8657, Email : s.k.wilson@strath.ac.uk

at leading order in the limit of small Biot number). We show that the effect of cooling the atmosphere is always to widen and deepen the rivulet, while the effect of heating the atmosphere is always to narrow and shallow it. We interpret our results as describing a slowly varying rivulet draining in the azimuthal direction from the top to the bottom of a large horizontal circular cylinder, and find that the behaviour of the rivulet is rather different on the upper and lower parts of the cylinder (i.e. for sessile and pendent rivulets). Specifically, the effect of strong cooling of the atmosphere is to produce a wide rivulet with finite uniform thickness on the upper part of the cylinder, but a deep rivulet with finite semi-width on the lower part of the cylinder. On the other hand, the effect of strong heating of the atmosphere is to produce a narrow and shallow rivulet everywhere except near the top and the bottom of the cylinder.

Keywords (from official list): Capillary Flows, Contact Lines, Spreading Films, Coating Flows.

I. INTRODUCTION

Gravity-driven rivulet flows are ubiquitous in a wide range of practical situations, including many industrial coating processes and geophysical flows. As a result in recent years there has been considerable work on the gravity-driven draining of an isothermal rivulet down an inclined substrate, much of it building on the pioneering analysis of steady unidirectional flow of Newtonian fluid down an inclined plane in the presence of significant surface-tension effects undertaken by Towell and Rothfeld [1]. Duffy and Moffatt [2] used the lubrication approximation employed by Allen and Biggin [3] to obtain analytically the leading-order solution in the special case when the cross-sectional profile of the rivulet in the direction transverse to the flow is thin. Duffy and Moffatt [2] calculated the shape of the rivulet (and, in particular, its width and maximum height) as a function of α, the angle of inclination of the substrate to the horizontal, for $0 \leq \alpha \leq \pi$. Duffy and Moffatt [2] also interpreted their results as describing the locally unidirectional flow down a locally planar substrate whose local slope α varies slowly in the flow-wise direction and, in particular, used them to describe the flow in the azimuthal direction round a large horizontal circular cylinder. Duffy and Moffatt's [2] approach has been used by Wilson and Duffy [4] to study the locally unidirectional flow of a rivulet down a slowly varying substrate with variation transverse to the direction of flow, and by Wilson, Duffy and Ross [5] to study the locally unidirectional flow of a rivulet of viscoplastic material down a slowly varying substrate. Taking a somewhat different approach Smith [6] and Duffy and Moffatt [7] obtained similarity solutions of the thin-film equations describing the steady draining of a slender non-uniform rivulet from a point source or to a point sink on an inclined plane in the cases of weak and strong surface-tension effects respectively.

However, in many situations one or more non-isothermal effects, including temperature dependence of various fluid properties such as surface tension, viscosity and density, as well as

evaporation effects, are significant. Despite its practical importance there has thus far been surprisingly little work on non-isothermal rivulet flow.

Holland, Duffy and Wilson [8] investigated the steady locally uniform (but not locally unidirectional) flow of a thin rivulet of a fluid with constant viscosity whose *surface tension* varies linearly with temperature down a slowly varying substrate that is either uniformly hotter or uniformly colder than the surrounding atmosphere. In particular, they found that the variation in surface tension drives a transverse flow that causes the fluid particles to spiral down the rivulet in helical vortices (absent in the corresponding isothermal problem). They also found that a single continuous rivulet can run from the top to the bottom of a large horizontal circular cylinder provided that the cylinder is either warmer or significantly cooler than the surrounding atmosphere, but that if it is only slightly cooler than the surrounding atmosphere then a continuous rivulet is possible only for a sufficiently small volume flux.

Recently Wilson and Duffy [9] studied the unsteady flow of a thin rivulet of fluid with constant surface tension whose *viscosity* varies with temperature down a substrate that is again either uniformly hotter or uniformly colder than the surrounding atmosphere. In particular, they derived the general nonlinear evolution equation for a thin film of fluid with an arbitrary dependence of viscosity on temperature. They then used this equation to show that at leading order in the limit of small Biot number the rivulet is isothermal, as expected, but that at leading order in the limit of large Biot number (in which the rivulet is not isothermal) the governing equation can, rather unexpectedly, always be reduced to that in the isothermal case with a suitable rescaling. These results were then used to give a complete description of steady flow of a slender rivulet in the limit of large Biot number in two situations in which the corresponding isothermal problem has previously been solved analytically, namely non-uniform flow down an inclined plane, and locally unidirectional flow down a slowly varying substrate. In particular, they found that if a suitably defined integral measure of the fluidity of the film is a decreasing

function of the temperature of the atmosphere (as it is for all three specific viscosity models they considered) then decreasing the temperature of the atmosphere always has the effect of making the rivulet wider and deeper. Wilson and Duffy [9] also review previous work on other thin-film flows of fluid with temperature-dependent viscosity, including the work by Goussis and Kelly [10] and Hwang and Weng [11] on the stability of a two-dimensional film draining down a uniformly heated or cooled inclined plane, and the work by Reisfeld and Bankoff [12], Wu and Hwang [13] and Oron, Davis and Bankoff [14] on the non-linear evolution of a film with surface-tension and van-der-Waals effects. There has also been considerable work on thin-film flows with a variety of other non-isothermal effects (see, for example, the excellent review by Oron, Davis and Bankoff [14] for further details).

The present paper continues the investigation of non-isothermal rivulet flow of a fluid with temperature-dependent viscosity by considering steady locally unidirectional gravity-driven draining of a thin rivulet of Newtonian fluid down a slowly varying substrate that is either uniformly hotter or uniformly colder than the surrounding atmosphere. We consider the situation in which the Biot number (and hence the variation of temperature across the rivulet) is small, but (in contrast to the situation studied by Wilson and Duffy [9]) in which the variation of viscosity with temperature is sufficiently strong that thermoviscosity effects appear at leading order in the limit of small Biot number.

II. PROBLEM FORMULATION

Consider initially the steady unidirectional gravity-driven draining of a thin symmetric rivulet of constant (but unknown) semi-width a of Newtonian fluid with prescribed positive volume flux $\bar{Q} > 0$ down a planar substrate inclined at an angle α ($0 \leq \alpha \leq \pi$) to the horizontal, shown in Fig. 1. We choose Cartesian axes $Oxyz$ as indicated in Fig. 1, with the x axis in the direction of flow and the y axis horizontal (transverse to the direction of flow) with respect

to which the substrate is denoted by $z = 0$. The velocity $\mathbf{u} = u(y,z)\mathbf{i}$, pressure $p = p(x,y,z)$ and temperature $T = T(x,y,z)$ of the fluid are governed by the familiar mass-conservation, Navier–Stokes and energy equations. The fluid is assumed to have constant density ρ, surface tension γ and thermal conductivity k_{th}, but a non-constant viscosity $\mu = \mu(T)$ that depends on temperature. On the solid substrate $z = 0$ the fluid velocity is zero and the uniform temperature is prescribed to be $T = T_0$. On the free surface $z = h(y)$ the usual normal and tangential stress balances, the energy balance

$$-k_{\text{th}} \nabla T \cdot \mathbf{n} = \alpha_{\text{th}} (T - T_\infty) \tag{1}$$

(where T_∞ denotes the uniform temperature of the surrounding atmosphere, α_{th} the surface heat-transfer coefficient and $\mathbf{n}$ the unit normal to the free surface) and the kinematic condition apply. At the edges of the rivulet $y = \pm a$ where $h = 0$ the contact angle takes the prescribed value β.

Three different viscosity models will be considered in the present work, namely the *linear* model

$$\mu(T) = \mu_0 - \lambda(T - T_0) \tag{2}$$

(valid only for $\mu > 0$, i.e. $\mu_0 > \lambda(T - T_0)$), the *exponential* model

$$\mu(T) = \mu_0 \exp\left[-\frac{\lambda(T - T_0)}{\mu_0}\right], \tag{3}$$

and the *Eyring* model

$$\mu(T) = \mu_0 \exp\left[\frac{\lambda T_0^2}{\mu_0}\left(\frac{1}{T} - \frac{1}{T_0}\right)\right]. \tag{4}$$

Note that all three models satisfy $\mu = \mu_0$ and $\mathrm{d}\mu/\mathrm{d}T = -\lambda$ at $T = T_0$, where λ is a prescribed positive constant, and hence all the models coincide up to and including $O(T - T_0)$ in the limit $T \to T_0$.

Analytical progress can be made by considering the case of a rivulet whose cross section is slender (with, in particular, $\beta \ll 1$), and thus we scale the system appropriately by writing

$$y = ly^*, \quad z = \beta l z^*, \quad h = \beta l h^*, \quad u = \frac{\rho g \beta^2 l^2}{\mu_0} u^*, \quad Q = \frac{\rho g \beta^3 l^4}{\mu_0} Q^*,$$
$$p = p_\infty + \rho g \beta l p^*, \quad \mu = \mu_0 \mu^*, \quad T = T_\infty + (T_0 - T_\infty) T^*, \tag{5}$$

where $l = (\gamma/\rho g)^{1/2}$ is the capillary length in which g denotes acceleration due to gravity, and p_∞ is the uniform pressure of the surrounding atmosphere. Note that for simplicity we have chosen μ_0, the viscosity of the fluid at the substrate temperature $T = T_0$, as the characteristic viscosity scale. This choice is most appropriate to experimental situations in which the temperature of the substrate is held fixed while other physical parameters are varied. An alternative choice more appropriate to experimental situations in which the temperature of the atmosphere is held fixed would be to use the viscosity of the fluid at the temperature of the atmosphere $T = T_\infty$ as the characteristic viscosity scale. [15] The star subscripts will be dropped immediately for clarity, and hereafter all quantities are non-dimensional unless it is stated otherwise.

The leading-order versions of the governing Navier–Stokes and energy equations are

$$0 = \sin\alpha + (\mu u_z)_z, \tag{6}$$

$$0 = -p_y, \tag{7}$$

$$0 = -p_z - \cos\alpha, \tag{8}$$

$$T_{zz} = 0, \tag{9}$$

showing that the steady flow is the consequence of a balance between gravity and viscous effects, that the pressure is hydrostatic, and that the transport of heat is dominated by diffusion in the z direction. These equations are to be integrated subject to the boundary conditions of no slip and prescribed temperature at the substrate $z = 0$,

$$u = 0, \quad T = 1, \tag{10}$$

balances of normal and tangential stress and an energy balance at the free surface $z = h(y)$,

$$p = -h'', \tag{11}$$

$$u_z = 0 \tag{12}$$

$$T_z + BT = 0, \tag{13}$$

where

$$B = \frac{\beta l \alpha_{\text{th}}}{k_{\text{th}}} \tag{14}$$

denotes the non-dimensional Biot number, and prescribed constant contact angle at the edges of the rivulet $y = \pm a$,

$$h = 0, \tag{15}$$

$$h' = \mp 1. \tag{16}$$

Primes denote differentiation with respect to argument. Note that the mass-conservation equation and the kinematic condition are satisfied identically.

Integrating (8) subject to (11) at $z = h$ yields

$$p = (h - z)\cos\alpha - h''. \tag{17}$$

Then (7) yields a third-order ordinary differential equation for h, namely

$$(h'' - h\cos\alpha)' = 0, \tag{18}$$

showing that the profile of the rivulet is determined by a simple balance between surface-tension and gravity effects. Solving (18) subject to (15) and (16) at $y = \pm a$ yields

$$h(y) = \begin{cases} \dfrac{\cosh ma - \cosh my}{m \sinh ma} & \text{if} \quad 0 \le \alpha < \pi/2, \\ \dfrac{a^2 - y^2}{2a} & \text{if} \quad \alpha = \pi/2, \\ \dfrac{\cos my - \cos ma}{m \sin ma} & \text{if} \quad \pi/2 < \alpha \le \pi, \end{cases} \tag{19}$$

where we have introduced the notation $m = |\cos\alpha|^{1/2}$, in agreement with the results of Duffy and Moffatt [2] in the isothermal case. In particular, the maximum thickness of the cross section of the rivulet, denoted by $h_{\rm m} = h(0)$, is given by

$$h_{\rm m} = \begin{cases} \dfrac{1}{m}\tanh\left(\dfrac{ma}{2}\right) & \text{if} \quad 0 \le \alpha < \pi/2, \\ \dfrac{a}{2} & \text{if} \quad \alpha = \pi/2, \\ \dfrac{1}{m}\tan\left(\dfrac{ma}{2}\right) & \text{if} \quad \pi/2 < \alpha \le \pi. \end{cases} \tag{20}$$

For future reference it is useful to note that if $a \to \infty$ in $0 \le \alpha < \pi/2$ then

$$h \sim \frac{1}{m}\left[1 - \mathrm{e}^{-m(a-|y|)}\right], \tag{21}$$

if $ma \to \pi$ in $\pi/2 < \alpha \le \pi$ then

$$h \sim \frac{1 + \cos my}{m(\pi - ma)} \to \infty, \tag{22}$$

while if $a \to 0$ then

$$h \sim \frac{a^2 - y^2}{2a} \to 0. \tag{23}$$

Integrating (9) twice subject to (10) at $z = 0$ and (13) at $z = h$ yields

$$T = 1 - \frac{Bz}{1 + Bh}. \tag{24}$$

Thus if we define an *effective thermoviscosity number* $\hat{V}$, a non-dimensional measure of the variation of viscosity with temperature, by

$$\hat{V} = \frac{\lambda(T_0 - T_\infty)B}{\mu_0} = \frac{\lambda(T_0 - T_\infty)\beta l \alpha_{\rm th}}{\mu_0 k_{\rm th}} \tag{25}$$

then the linear model (2) yields

$$\mu = 1 - \frac{\hat{V}}{B}(T - 1) = 1 + \frac{\hat{V}z}{1 + Bh} \tag{26}$$

(valid only for $\mu > 0$, i.e. $(B + \hat{V})h_{\rm m} > -1$), while the exponential model (3) yields

$$\mu = \exp\left(-\frac{\hat{V}}{B}(T - 1)\right) = \exp\left(\frac{\hat{V}z}{1 + Bh}\right), \tag{27}$$

and the Eyring model (4) yields

$$\mu = \exp\left(-\frac{T_0\hat{V}(T-1)}{B(T_0+(T_0-T_\infty)(T-1))}\right) = \exp\left(\frac{\hat{V}_\mathrm{m}\hat{V}z}{\hat{V}_\mathrm{m}(1+Bh)-B\hat{V}z}\right), \tag{28}$$

where we have defined $\hat{V}_\mathrm{m} = \lambda T_0 B/\mu_0 = \lambda T_0 \beta l \alpha_\mathrm{th}/\mu_0 k_\mathrm{th}$. Note that by definition $\hat{V}_\mathrm{m} > 0$ and $\hat{V}_\mathrm{m} > \hat{V}$. The effective thermoviscosity number $\hat{V}$ plays a role analogous to that played by the effective Marangoni number used by Holland, Duffy and Wilson [8] for the corresponding problem when thermocapillary effects are significant [16], but differs from the thermoviscosity number $V = \hat{V}/B$ introduced by Wilson and Duffy [9] by a factor of B. Positive (negative) values of $\hat{V}$ correspond to $T_0 > T_\infty$ ($T_0 < T_\infty$), i.e. to situations in which the atmosphere is colder (hotter) than the substrate and in which the viscosity at the free surface is accordingly greater than (less than) the viscosity at the substrate. The case $\hat{V} = 0$ corresponds to the isothermal problem $T_0 = T_\infty$ in which the viscosity is constant, $\mu \equiv 1$. Since in practice the Biot number B is often small we shall hereafter restrict our attention to the solution in the limit $B \to 0$ for fixed $\hat{V}$ (and for the Eyring model also fixed $\hat{V}_\mathrm{m}$). In this limit the linear model reduces to simply

$$\mu = 1 + \hat{V}z \tag{29}$$

(valid only for $\hat{V}h_\mathrm{m} > -1$), while both the exponential and the Eyring models reduce to

$$\mu = \exp(\hat{V}z). \tag{30}$$

Since the exponential and Eyring models coincide at leading order we shall hereafter refer to the "exponential/Eyring" model. Note that all the models coincide up to and including $O(\hat{V})$ in the limit $\hat{V} \to 0$. It is important to realise that while the variation of temperature across the rivulet is small in the limit $B \to 0$ (specifically $T = 1 + O(B)$), when $\hat{V} = O(1)$ the variation of viscosity with temperature is sufficiently strong that thermoviscosity effects appear at leading order. This is fundamentally different from the situation considered by Wilson and Duffy [9]

in which $V = O(1)$ and hence $\hat{V} = O(B)$, in which viscosity is constant at leading order in the limit $B \to 0$.

Integrating (6) once subject to (10) at $z = 0$ yields

$$u = \sin\alpha \int_0^z \frac{h - \tilde{z}}{\mu} \, \mathrm{d}\tilde{z}. \tag{31}$$

Once u has been calculated from (31) the local flux $\bar{u} = \bar{u}(y)$ is given by

$$\bar{u} = \int_0^h u \, \mathrm{d}z = \frac{\sin\alpha}{3} f h^3, \tag{32}$$

where the function $f = f(x, y)$ is the *fluidity* of the film defined by

$$f = \frac{3}{h^3} \int_0^h \int_0^z \frac{h - \tilde{z}}{\mu(T)} \, \mathrm{d}\tilde{z} \, \mathrm{d}z, \tag{33}$$

and hence the flux of fluid down the rivulet, Q, is given by

$$Q = \int_{-a}^{+a} \bar{u} \, \mathrm{d}y = \frac{\sin\alpha}{3} \int_{-a}^{+a} f h^3 \, \mathrm{d}y. \tag{34}$$

For the linear model (29) we obtain

$$u = \frac{\sin\alpha}{\hat{V}^2} \left[-\hat{V}z + (1 + \hat{V}h) \log(1 + \hat{V}z) \right] \tag{35}$$

and the fluidity $f = f(\hat{V}h)$ is given by [18]

$$f(\hat{V}h) = \frac{3}{2(\hat{V}h)^3} \left[-\hat{V}h(2 + 3\hat{V}h) + 2(1 + \hat{V}h)^2 \log(1 + \hat{V}h) \right] \tag{36}$$

for $\hat{V}h > -1$, while for the exponential/Eyring model (30) we obtain

$$u = \frac{\sin\alpha}{\hat{V}^2} \left[\hat{V}h - 1 + (1 + \hat{V}z - \hat{V}h) \exp(-\hat{V}z) \right] \tag{37}$$

and the fluidity $f = f(\hat{V}h)$ is given by

$$f(\hat{V}h) = \frac{3}{(\hat{V}h)^3} \left[(\hat{V}h - 1)^2 + 1 - 2\exp(-\hat{V}h) \right]. \tag{38}$$

For both models the expression for Q is obtained by substituting for h from (19) into (34) using the appropriate form of $f(\hat{V}h)$. In general this expression is very lengthy and is therefore omitted for brevity. However, simplified expressions are obtained in the special case of flow down a vertical substrate ($\alpha = \pi/2$) and in the isothermal case ($\hat{V} = 0$). When $\alpha = \pi/2$ we obtain

$$Q\hat{V}^4 = \frac{8\hat{V}a}{15}\left[\frac{(2+\hat{V}a)^5}{\hat{V}a}\right]^{1/2} \tanh^{-1}\left[\left(\frac{\hat{V}a}{2+\hat{V}a}\right)^{1/2}\right] - \frac{8\hat{V}a}{225}\left[23(\hat{V}a)^2 + 70\hat{V}a + 60\right] \tag{39}$$

(valid only for $\hat{V}a > -2$) for the linear model (29), and

$$Q\hat{V}^4 = \frac{4\hat{V}a}{15}\left[(\hat{V}a)^2 - 5\hat{V}a + 15\right] - 2\hat{V}a\left(-\frac{2\pi}{\hat{V}a}\right)^{1/2} \exp\left(-\frac{\hat{V}a}{2}\right) \operatorname{erf}\left[\left(-\frac{\hat{V}a}{2}\right)^{1/2}\right] \tag{40}$$

for the exponential/Eyring model (30). Figure 2 shows $Q\hat{V}^4$ given by both (39) and (40) plotted as functions of $\hat{V}a$. For future reference it is useful to note that in this case for both models

$$Q\hat{V}^4 = \frac{4}{105}(\hat{V}a)^4 - \frac{4}{945}(\hat{V}a)^5 + O(\hat{V}a)^6 \tag{41}$$

as $\hat{V}a \to 0$, for the linear model

$$Q\hat{V}^4 \sim \frac{8(\hat{V}a)^3}{225}\left[\frac{15}{2}\log(2\hat{V}a) - 23\right] \tag{42}$$

as $\hat{V}a \to \infty$ and $Q\hat{V}^4 \to 64/75$ as $\hat{V}a \to -2^+$, while for the exponential/Eyring model $Q\hat{V}^4 \sim 4(\hat{V}a)^3/15$ as $\hat{V}a \to \infty$ and

$$Q\hat{V}^4 \sim 4\sqrt{\pi}\left(-\frac{\hat{V}a}{2}\right)^{1/2} \exp\left(-\frac{\hat{V}a}{2}\right) \tag{43}$$

as $\hat{V}a \to -\infty$. On the other hand, when $\hat{V} = 0$ we obtain

$$Q = \frac{\sin\alpha}{9m^4}F(ma), \tag{44}$$

where we have defined

$$F(ma) = \begin{cases} 15ma\coth^3 ma - 15\coth^2 ma - 9ma\coth ma + 4 & \text{if} \quad 0 \le \alpha < \pi/2, \\ \dfrac{12}{35}(ma)^4 & \text{if} \quad \alpha = \pi/2, \\ -15ma\cot^3 ma + 15\cot^2 ma - 9ma\cot ma + 4 & \text{if} \quad \pi/2 < \alpha \le \pi, \end{cases} \tag{45}$$

recovering the corresponding results obtained by Duffy and Moffatt [2] in the isothermal case. (Note that in the case $\alpha = \pi/2$ we have $m = 0$ and the factors of m^4 in (44) must be cancelled before setting $\alpha = \pi/2$.)

For any prescribed positive value of the flux, $\bar{Q} > 0$, the possible rivulet semi-widths are the positive solutions for a of the equation $Q = \bar{Q}$, where Q is given by (34). Once a is known h is given explicitly by (19). In practice since the algebra required to calculate Q is rather lengthy we used the symbolic algebra package MAPLE V running on a SUN ULTRA 10 to perform the analytical evaluation of Q from (34) as well as the subsequent numerical calculation of a from the algebraic equation $Q = \bar{Q}$.

Clearly the effect of cooling the atmosphere ($\hat{V} > 0$) will be to cool the fluid and hence to increase its viscosity and therefore decrease its velocity. Since the flux is constant this means that cooling the atmosphere must increase the cross-sectional area of the rivulet. Conversely heating the atmosphere ($\hat{V} < 0$) must decrease the cross-sectional area of the rivulet. In fact, stronger results hold, namely that the effect of cooling the atmosphere is always to *widen and deepen* the rivulet, and that the effect of heating the atmosphere is always to *narrow and shallow* it. These results can be shown as follows. When $0 < \alpha < \pi$ it is straightforward to show from (19) that $\partial h/\partial a > 0$, and from (32) with either (36) or (38) that $\partial \bar{u}/\partial \hat{V} < 0$ and $\partial \bar{u}/\partial h > 0$ for both the linear and exponential/Eyring models, and so we can immediately deduce from (34) with $Q = \bar{Q}$ that

$$\frac{\partial a}{\partial \hat{V}} = -\frac{\displaystyle\int_{-a}^{+a} \frac{\partial \bar{u}}{\partial \hat{V}}\,\mathrm{d}y}{\displaystyle\int_{-a}^{+a} \frac{\partial \bar{u}}{\partial h}\frac{\partial h}{\partial a}\,\mathrm{d}y} > 0, \tag{46}$$

and then from (20) that $\partial h_{\mathrm{m}}/\partial \hat{V} > 0$. In other words, except when $\alpha = 0$ or $\alpha = \pi$, both a and h_{m} are monotonically increasing functions of $\hat{V}$, and so the general results described above hold. Nevertheless, as we shall see subsequently, the behaviour of the rivulet is rather different for $0 \leq \alpha < \pi/2$, $\alpha = \pi/2$ and $\pi/2 < \alpha \leq \pi$.

So far the analysis has been restricted to strictly unidirectional flow but, as Duffy and Moffatt [2] describe, this solution is also the leading-order approximation to the local behaviour of a rivulet with non-uniform width draining down a non-planar cylindrical substrate, where α now represents the *local* inclination of the substrate to the horizontal, provided that α varies sufficiently slowly, i.e. provided that the longitudinal aspect ratio $\epsilon = l\beta/R$, the reduced Reynolds number $\rho^2 g\beta^4 l^4/\mu_0^2 R$, and the reduced Peclet number $\rho^2 cg\beta^4 l^4/k_{\rm th}\mu_0 R$ (where R is a typical radius of curvature of the substrate) are sufficiently small. Thus we shall interpret the results given subsequently as describing a slowly varying rivulet draining in the azimuthal direction from the top ($\alpha = 0$) to the bottom ($\alpha = \pi$) of a large horizontal circular cylinder as sketched in Fig. 3. As Wilson and Duffy [4] showed, in the isothermal case there are multiple branches of solutions for a in $\pi/2 < \alpha \leq \pi$, but of these only the one that connects smoothly with the solution in $0 \leq \alpha \leq \pi/2$ is physically realisable. We shall henceforth restrict our attention to this latter type of solution.

In the remainder of this paper we shall concentrate our attention on the more realistic exponential/Eyring model (30) for brevity.

III. RESULTS FOR THE EXPONENTIAL/EYRING MODEL

Figures 4, 5 and 6 show numerically calculated values of a and $h_{\rm m}$ plotted as functions of α/π for a range of values of $\hat{V}$ when $\bar{Q} = 1$, a range of values of $\bar{Q}$ when $\hat{V} = 1$, and a range of values of $\bar{Q}$ when $\hat{V} = -1$, respectively. In particular, these figures confirm that a and $h_{\rm m}$ are monotonically increasing functions of $\hat{V}$. The figures also show that the behaviour of the rivulet is rather different on the upper and lower parts of the cylinder. Specifically, they show that the effect of strong cooling of the atmosphere $\hat{V} \to \infty$, in which the viscosity of the fluid is large so that the velocity is small and hence the cross-sectional area of the rivulet is large, is to produce a wide sessile rivulet with finite thickness on the upper part of the cylinder,

but a deep pendent rivulet with finite semi-width on the lower part of the cylinder. On the other hand, the effect of strong heating of the atmosphere $\hat{V} \to -\infty$, in which the viscosity of the fluid is small so that the velocity is large and hence the cross-sectional area of the rivulet is small, is to produce a narrow and shallow rivulet everywhere except near the top and the bottom of the cylinder. All the qualitative features of the numerical results are captured by the asymptotic results in the limits $\alpha \to 0$, $\alpha \to \pi$, $\hat{V} \to 0$, $\hat{V} \to \infty$, $\hat{V} \to -\infty$, $\bar{Q} \to 0$ and $\bar{Q} \to \infty$ presented below. The corresponding asymptotic results for the less realistic linear model (29) are given in Appendix A for completeness. For brevity only the final asymptotic results are given below, but in Appendix B we give the details of the analysis in one specific case (namely the limit $\bar{Q} \to \infty$) in order to indicate how the results were obtained.

A. The limit $\alpha \to 0$

In the limit $\alpha \to 0$ we have $a \to \infty$, and substituting (21) into (34) reveals that

$$a \sim \frac{3\bar{Q}}{2f(\hat{V})\alpha} \to \infty, \quad h_{\mathrm{m}} \sim 1 + \frac{\alpha^2}{4}, \tag{47}$$

where the function $f(\hat{V})$ is given by (38). The function $f(\hat{V})$ is plotted in Fig. 7, and satisfies

$$f = \frac{6\exp(-\hat{V})}{(-\hat{V})^3} + O\left(\frac{1}{\hat{V}}\right) \quad \text{as} \quad \hat{V} \to -\infty, \tag{48}$$

$$f = 1 - \frac{\hat{V}}{4} + O(\hat{V}^2) \quad \text{as} \quad \hat{V} \to 0, \tag{49}$$

$$f = \frac{3}{\hat{V}} + O\left(\frac{1}{\hat{V}^2}\right) \quad \text{as} \quad \hat{V} \to \infty. \tag{50}$$

In particular, when $\hat{V} = 0$ we recover the corresponding results in the isothermal case obtained by Duffy and Moffatt [2]. Whatever the value of $\hat{V}$, we have $a \to \infty$ and $h_{\mathrm{m}} \to 1$ with h given by (21), and so near the top of the cylinder the rivulet always becomes wide with height approaching unity everywhere except in boundary layers near $y = \pm a$.

B. The limit $\alpha \to \pi$

In the limit $\alpha \to \pi$ we have $a \to \pi$, and substituting (22) into (34) using (38) reveals that the behaviour of the solution depends on whether $\hat{V} > 0$, $\hat{V} = 0$ or $\hat{V} < 0$. When $\hat{V} > 0$ we have

$$a \sim \pi - \left[\frac{3\pi(\pi-\alpha)}{\bar{Q}\hat{V}}\right]^{1/2}, \quad h_{\mathrm{m}} \sim \left[\frac{4\bar{Q}\hat{V}}{3\pi(\pi-\alpha)}\right]^{1/2} \to \infty, \tag{51}$$

when $\hat{V} = 0$ we have

$$a \sim \pi - \left[\frac{5\pi(\pi-\alpha)}{3\bar{Q}}\right]^{1/3}, \quad h_{\mathrm{m}} \sim \left[\frac{24\bar{Q}}{5\pi(\pi-\alpha)}\right]^{1/3} \to \infty, \tag{52}$$

recovering the corresponding results in the isothermal case obtained by Duffy and Moffatt [2], and when $\hat{V} < 0$ we have

$$a \sim \pi - 4(-\hat{V})\left[-\mathrm{W}\left(-\frac{32\pi(\pi-\alpha)^2}{\bar{Q}^2\hat{V}^6}\right)\right]^{-1} \sim \pi - \frac{2(-\hat{V})}{[-\log(\pi-\alpha)]}, \tag{53}$$

$$h_{\mathrm{m}} \sim \frac{1}{2(-\hat{V})}\left[-\mathrm{W}\left(-\frac{32\pi(\pi-\alpha)^2}{\bar{Q}^2\hat{V}^6}\right)\right] \sim \frac{[-\log(\pi-\alpha)]}{(-\hat{V})} \to \infty, \tag{54}$$

where $\mathrm{W} = \mathrm{W}(x)$ is Lambert's W function which satisfies $\mathrm{W}\exp(\mathrm{W}) = x$. Relevant properties of W are summarised in Appendix C. In particular, in (53) and (54) we have used the fact that $\mathrm{W}(x) \sim \log(-x)$ as $x \to 0^-$ on the relevant branch of W. Whatever the value of $\hat{V}$, we have $a \to \pi$ and $h_{\mathrm{m}} \to \infty$ with h given by (22), and so near the bottom of the cylinder the rivulet always becomes deep with semi-width approaching π.

C. The limit $\hat{V} \to 0$

In the limit of weak cooling or heating of the atmosphere $\hat{V} \to 0$ the linear and exponential/Eyring models coincide up to and including $O(\hat{V})$, and so for *both* models we obtain

$$\bar{u} = \frac{\sin\alpha}{3}\left[h^3 - \frac{h^4}{4}\hat{V} + O(\hat{V}^2)\right]. \tag{55}$$

Seeking solutions for h and a as regular expansions in powers of $\hat{V}$ in the form

$$h(y) = h_0(y) + \hat{V}h_1(y) + O(\hat{V}^2), \quad a = a_0 + \hat{V}a_1 + O(\hat{V}^2), \tag{56}$$

where $h_0 = h_0(y)$ and a_0 are the solutions in the isothermal case obtained by Duffy and Moffatt [2], we find that $h_1 = h_1(y)$ and a_1 satisfy

$$(h_1'' - h_1 \cos\alpha)' = 0 \tag{57}$$

subject to the boundary conditions

$$a_1 h_0'(a_0) + h_1(a_0) = 0, \tag{58}$$

$$a_1 h_0''(a_0) + h_1'(a_0) = 0, \tag{59}$$

$$h_1'(0) = 0, \tag{60}$$

and the flux condition

$$\int_{-a_0}^{+a_0} h_0^2 h_1 - \frac{h_0^4}{12}\,\mathrm{d}y = 0. \tag{61}$$

Hence we find that $h_1(y) = a_1 H_1(y)$, where H_1 is given by

$$H_1(y) = \begin{cases} \dfrac{\cosh ma_0 \cosh my - 1}{\sinh^2 ma_0} & \text{if} \quad 0 \le \alpha < \pi/2, \\ \dfrac{a_0^2 + y^2}{2a_0^2} & \text{if} \quad \alpha = \pi/2, \\ \dfrac{1 - \cos ma_0 \cos my}{\sin^2 ma_0} & \text{if} \quad \pi/2 < \alpha \le \pi, \end{cases} \tag{62}$$

and so from (61)

$$a_1 = \frac{\displaystyle\int_{-a_0}^{+a_0} h_0^4\,\mathrm{d}y}{12\displaystyle\int_{-a_0}^{+a_0} h_0^2 H_1\,\mathrm{d}y}. \tag{63}$$

Evaluating (63) reveals that

$$a_1 = \frac{24ma_0C^4 - 50C^3S + 72ma_0C^2 - 55CS + 9ma_0}{48m^2(2C^3S - 12ma_0C^2 + 13CS - 3ma_0)} \tag{64}$$

(where $C = \cosh ma_0$ and $S = \sinh ma_0$) if $0 \le \alpha < \pi/2$,

$$a_1 = \frac{a_0^2}{36} \tag{65}$$

if $\alpha = \pi/2$, and

$$a_1 = -\frac{24ma_0C^4 - 50C^3S + 72ma_0C^2 - 55CS + 9ma_0}{48m^2(2C^3S - 12ma_0C^2 + 13CS - 3ma_0)} \tag{66}$$

(where $C = \cos ma_0$ and $S = \sin ma_0$) if $\pi/2 < \alpha \leq \pi$. Notice that (65) and (66) can be recovered from (64) by letting $m \to 0$ and replacing m with im, respectively. If we write $h_{\rm m} = h_{\rm m0} + \hat{V} h_{\rm m1} + O(\hat{V}^2)$ then $h_{\rm m0} = h_0(0)$ and $h_{\rm m1} = h_1(0) = a_1 H_1(0)$, where

$$H_1(0) = \begin{cases} \dfrac{1}{2}\operatorname{sech}^2\left(\dfrac{ma_0}{2}\right) & \text{if} \quad 0 \leq \alpha < \pi/2, \\ \dfrac{1}{2} & \text{if} \quad \alpha = \pi/2, \\ \dfrac{1}{2}\sec^2\left(\dfrac{ma_0}{2}\right) & \text{if} \quad \pi/2 < \alpha \leq \pi. \end{cases} \tag{67}$$

Figure 8 shows a_1 and $h_{\rm m1}$ plotted as functions of α/π in the case $\bar{Q} = 1$. In particular, Fig. 8 shows that $a_1 > 0$ and $h_{\rm m1} > 0$ for all $0 \leq \alpha \leq \pi$. Thus the effect of weak cooling of the atmosphere ($\hat{V} \to 0^+$) is always to widen and deepen the rivulet, while the effect of weak heating of the atmosphere ($\hat{V} \to 0^-$) is always to narrow and shallow it, in agreement with the general results established earlier. Note that $a_1 \sim a_0/4 \to \infty$, $h_{\rm m1} \sim a_0 \exp(-a_0)/2 \to 0$ as $\alpha \to 0$ ($a_0 \to \infty$), that $a_1 = a_0^2/36$, $h_{\rm m1} = a_0^2/72$ at $\alpha = \pi/2$ ($a_0 = (105\bar{Q}/4)^{1/4}$), and that $a_1 = 7/48 - (\pi - a_0)^2/20 + O(\pi - a_0)^4$, $h_{\rm m1} \sim (7/24)(\pi - a_0)^{-2} \to \infty$ as $\alpha \to \pi$ ($a_0 \to \pi$), and hence that these solutions are uniformly valid near $\alpha = 0$ but not near $\alpha = \pi$.

D. The limit $\hat{V} \to \infty$

In the limit of strong cooling of the atmosphere $\hat{V} \to \infty$ the behaviour of the solution depends on whether $0 \leq \alpha < \pi/2$, $\alpha = \pi/2$ or $\pi/2 < \alpha \leq \pi$. In $0 \leq \alpha < \pi/2$ we have $a \to \infty$, and substituting (21) into (34) using (38) yields

$$a \sim \frac{\bar{Q}\hat{V}m^2}{2\sin\alpha} \to \infty, \quad h_{\rm m} \sim \frac{1}{m}; \tag{68}$$

at $\alpha = \pi/2$ we have $a \to \infty$, and (40) yields

$$a \sim \left(\frac{15\bar{Q}\hat{V}}{4}\right)^{1/3} \to \infty, \quad h_{\rm m} \sim \frac{1}{2}\left(\frac{15\bar{Q}\hat{V}}{4}\right)^{1/3} \to \infty; \tag{69}$$

and in $\pi/2 < \alpha \leq \pi/2$ we have $ma \to \pi$, and substituting (22) into (34) using (38) yields

$$a \sim \frac{\pi}{m} - \frac{1}{m^2}\left(\frac{3\pi\sin\alpha}{\bar{Q}\hat{V}m}\right)^{1/2}, \quad h_{\rm m} \sim \left(\frac{4\bar{Q}\hat{V}m}{3\pi\sin\alpha}\right)^{1/2} \to \infty. \tag{70}$$

Thus, in $0 \leq \alpha < \pi/2$ we have $a = O(\hat{V})$ and $h_{\rm m} = O(1)$, while in $\pi/2 < \alpha \leq \pi$ we have $a = O(1)$ and $h_{\rm m} = O(\hat{V}^{1/2})$. The adjustments between these two different types of asymptotic behaviour occur via boundary layers near $\alpha = \pi/2$ of thickness $O(\hat{V}^{-2/3})$. Thus the effect of strong cooling of the atmosphere is to produce a wide rivulet on the upper part of the cylinder ($0 \leq \alpha \leq \pi/2$) and a deep rivulet on the lower part of the cylinder ($\pi/2 \leq \alpha \leq \pi$), in agreement with the general result established earlier. Note that these leading-order solutions are uniformly valid near both $\alpha = 0$ and $\alpha = \pi$.

E. The limit $\hat{V} \to -\infty$

In the limit of strong heating of the atmosphere $\hat{V} \to -\infty$ we have $a \to 0$ and substituting (23) into (34) using (38) reveals that

$$a \sim \frac{1}{(-\hat{V})} \mathrm{W}\left(\frac{\bar{Q}^2 \hat{V}^8}{8\pi \sin^2\alpha}\right) \sim \frac{8}{(-\hat{V})} \log(-\hat{V}) \to 0 \tag{71}$$

and

$$h_{\rm m} \sim \frac{1}{2(-\hat{V})} \mathrm{W}\left(\frac{\bar{Q}^2 \hat{V}^8}{8\pi \sin^2\alpha}\right) \sim \frac{4}{(-\hat{V})} \log(-\hat{V}) \to 0, \tag{72}$$

where in (71) and (72) we have used the fact that $\mathrm{W}(x) \sim \log x$ as $x \to \infty$. Thus the effect of strong heating of the atmosphere is to produce a narrow and shallow rivulet, in agreement with the general result established earlier. Note that these leading-order solutions are not uniformly valid near either $\alpha = 0$ or $\alpha = \pi$.

F. The limit $\bar{Q} \to 0$

In the limit of small flux $\bar{Q} \to 0$ we have $a \to 0$ (and hence $h \to 0$) and, since the linear and exponential/Eyring models coincide up to and including $O(h^4)$ in the limit $h \to 0$, for *both* models we obtain

$$\bar{u} = \frac{\sin\alpha}{3}\left[h^3 - \frac{\hat{V}}{4}h^4 + O(h^5)\right]. \tag{73}$$

Hence substituting (23) into (34) using (73) reveals that

$$a = \left(\frac{105\bar{Q}}{4\sin\alpha}\right)^{1/4} + \frac{\hat{V}}{36}\left(\frac{105\bar{Q}}{4\sin\alpha}\right)^{1/2} + O(\bar{Q}^{3/4}) \tag{74}$$

and

$$h_{\rm m} = \frac{1}{2}\left(\frac{105\bar{Q}}{4\sin\alpha}\right)^{1/4} + \frac{\hat{V}}{72}\left(\frac{105\bar{Q}}{4\sin\alpha}\right)^{1/2} + O(\bar{Q}^{3/4}). \tag{75}$$

In the case $\hat{V} = 0$ we recover the corresponding results in the isothermal case obtained by Holland, Duffy and Wilson [8]. Thus, whatever the value of $\hat{V}$, a rivulet with small flux is narrow and shallow. Note that these solutions are not uniformly valid near either $\alpha = 0$ or $\alpha = \pi$.

G. The limit $\bar{Q} \to \infty$

In the limit of large flux $\bar{Q} \to \infty$ the behaviour of the solution depends on whether $\hat{V} > 0$, $\hat{V} = 0$ or $\hat{V} < 0$ *and* on whether $0 \le \alpha < \pi/2$, $\alpha = \pi/2$ or $\pi/2 < \alpha \le \pi$. When $\hat{V} > 0$ we have

$$a \sim \begin{cases} \dfrac{3\bar{Q}m^3}{2f(\hat{V}/m)\sin\alpha} \to \infty & \text{if} \quad 0 \le \alpha < \pi/2, \\ \left(\dfrac{15\bar{Q}\hat{V}}{4}\right)^{1/3} \to \infty & \text{if} \quad \alpha = \pi/2, \\ \dfrac{\pi}{m} - \dfrac{1}{m^2}\left(\dfrac{3\pi\sin\alpha}{\bar{Q}\hat{V}m}\right)^{1/2} & \text{if} \quad \pi/2 < \alpha \le \pi, \end{cases} \tag{76}$$

where the function $f(\hat{V}/m)$ is given by (38) and

$$h_{\rm m} \sim \begin{cases} \dfrac{1}{m} & \text{if} \quad 0 \le \alpha < \pi/2, \\ \dfrac{1}{2}\left(\dfrac{15\bar{Q}\hat{V}}{4}\right)^{1/3} \to \infty & \text{if} \quad \alpha = \pi/2, \\ \left(\dfrac{4\bar{Q}\hat{V}m}{3\pi\sin\alpha}\right)^{1/2} \to \infty & \text{if} \quad \pi/2 < \alpha \le \pi. \end{cases} \tag{77}$$

When $\hat{V}=0$ we have

$$a \sim \begin{cases} \dfrac{3\bar{Q}m^3}{2\sin\alpha} \to \infty & \text{if} \quad 0 \le \alpha < \pi/2, \\ \left(\dfrac{105\bar{Q}}{4}\right)^{1/4} \to \infty & \text{if} \quad \alpha = \pi/2, \\ \dfrac{\pi}{m} - \dfrac{1}{m^2}\left(\dfrac{5\pi\sin\alpha}{3\bar{Q}m}\right)^{1/3} & \text{if} \quad \pi/2 < \alpha \le \pi, \end{cases} \tag{78}$$

and

$$h_{\mathrm{m}} \sim \begin{cases} \dfrac{1}{m} & \text{if} \quad 0 \le \alpha < \pi/2, \\ \dfrac{1}{2}\left(\dfrac{105\bar{Q}}{4}\right)^{1/4} \to \infty & \text{if} \quad \alpha = \pi/2, \\ \left(\dfrac{24\bar{Q}m}{5\pi\sin\alpha}\right)^{1/3} \to \infty & \text{if} \quad \pi/2 < \alpha \le \pi, \end{cases} \tag{79}$$

recovering the corresponding results in the isothermal case obtained by Holland, Duffy and Wilson [8]. When $\hat{V}<0$ we have

$$a \sim \begin{cases} \dfrac{3\bar{Q}m^3}{2f(\hat{V}/m)\sin\alpha} \to \infty & \text{if} \quad 0 \le \alpha < \pi/2, \\ \dfrac{1}{(-\hat{V})}\mathrm{W}\left(\dfrac{\bar{Q}^2\hat{V}^8}{8\pi}\right) \sim \dfrac{2}{(-\hat{V})}\log\bar{Q} \to \infty & \text{if} \quad \alpha = \pi/2, \\ \dfrac{\pi}{m} - \dfrac{4(-\hat{V})}{m^2}\left[-\mathrm{W}\left(-\dfrac{32\pi\sin^2\alpha}{\bar{Q}^2\hat{V}^6m^2}\right)\right]^{-1} \sim \dfrac{\pi}{m} - \dfrac{2(-\hat{V})}{m^2}(\log\bar{Q})^{-1} & \text{if} \quad \pi/2 < \alpha \le \pi, \end{cases} \tag{80}$$

where the function $f(\hat{V}/m)$ is again given by (38) and

$$h_{\mathrm{m}} \sim \begin{cases} \dfrac{1}{m} & \text{if} \quad 0 \le \alpha < \pi/2, \\ \dfrac{1}{2(-\hat{V})}\mathrm{W}\left(\dfrac{\bar{Q}^2\hat{V}^8}{8\pi}\right) \sim \dfrac{1}{(-\hat{V})}\log\bar{Q} \to \infty & \text{if} \quad \alpha = \pi/2, \\ \dfrac{1}{2(-\hat{V})}\left[-\mathrm{W}\left(-\dfrac{32\pi\sin^2\alpha}{\bar{Q}^2\hat{V}^6m^2}\right)\right] \sim \dfrac{1}{(-\hat{V})}\log\bar{Q} \to \infty & \text{if} \quad \pi/2 < \alpha \le \pi. \end{cases} \tag{81}$$

Thus, in $0 \le \alpha < \pi/2$ we have $a = O(\bar{Q})$ and $h_{\mathrm{m}} = O(1)$ for all $\hat{V}$, while in $\pi/2 < \alpha \le \pi$ we have $a = O(1)$ for all $\hat{V}$ together with $h_{\mathrm{m}} = O(\bar{Q}^{1/2})$ when $\hat{V} > 0$, $h_{\mathrm{m}} = O(\bar{Q}^{1/3})$ when $\hat{V} = 0$, and $h_{\mathrm{m}} = O(\log\bar{Q})$ when $\hat{V} < 0$. The adjustments between these different types of asymptotic behaviour occur via boundary layers near $\alpha = \pi/2$ of thickness $O(\bar{Q}^{-2/3})$ when

$\hat{V} > 0$ and $O(\bar{Q}^{-1/2})$ when $\hat{V} = 0$. When $\hat{V} < 0$ the situation is a little more complicated. In this case the boundary layers in a have thickness $O(\log \bar{Q}/\bar{Q})$ as $\alpha \to \pi/2^-$ and $O(\log \bar{Q})^{-2}$ as $\alpha \to \pi/2^+$, while the boundary layer in h_{m} has thickness $O(\log \bar{Q})^{-2}$ as $\alpha \to \pi/2^-$; at leading order there is no boundary layer in h_{m} as $\alpha \to \pi/2^+$ in this case. Thus, whatever the value of $\hat{V}$, a rivulet with large flux is wide on the upper part of the cylinder ($0 \leq \alpha \leq \pi/2$) and deep on the lower part of the cylinder ($\pi/2 \leq \alpha \leq \pi$). Note that these leading-order solutions are uniformly valid near both $\alpha = 0$ and $\alpha = \pi$.

IV. CONCLUSIONS

We used the lubrication approximation to investigate the steady locally unidirectional gravity-driven draining of a thin rivulet of Newtonian fluid with temperature-dependent viscosity down a slowly varying substrate that is either uniformly hotter or uniformly colder than the surrounding atmosphere. We considered the situation in which the Biot number B (and hence the variation of temperature across the rivulet) is small, but in which the variation of viscosity with temperature is sufficiently strong that thermoviscosity effects appear at leading order in the limit $B \to 0$. Three different models for the dependence of viscosity on temperature (specifically, the linear, exponential and Eyring models) were considered, but our attention was concentrated on the more realistic exponential and Eyring models (which coincide at leading order in the limit $B \to 0$). We showed that the effect of cooling the atmosphere ($\hat{V} > 0$) is always to widen and deepen the rivulet, while the effect of heating the atmosphere ($\hat{V} < 0$) is always to narrow and shallow it. We interpreted our results as describing a slowly varying rivulet draining in the azimuthal direction from the top to the bottom of a large horizontal circular cylinder, and found that the behaviour of the rivulet is rather different on the upper and lower parts of the cylinder (i.e. for sessile and pendent rivulets). Specifically, the effect of strong cooling of the atmosphere ($\hat{V} \to \infty$) is to produce a wide rivulet with uniform thickness

approaching $1/(\cos\alpha)^{1/2}$ on the upper part of the cylinder, but a deep rivulet with semi-width approaching $\pi/|\cos\alpha|^{1/2}$ on the lower part of the cylinder. On the other hand, the effect of strong heating of the atmosphere ($\hat{V} \to -\infty$) is to produce a narrow and shallow rivulet everywhere except near the top and the bottom of the cylinder.

ACKNOWLEDGEMENTS

The first author (SKW) gratefully acknowledges the financial support of the Leverhulme Trust via a Research Fellowship. Both authors wish to thank Prof. A. D. Fitt (Faculty of Mathematical Studies, University of Southampton) for bringing the present problem to their attention.

APPENDIX A: ASYMPTOTIC RESULTS FOR THE LINEAR MODEL

In this appendix we provide the asymptotic results for the linear model (29) corresponding to those for the exponential/Eyring model (30) given in Sec. III. All the details of the derivations, which broadly follow those for the exponential/Eyring model, are omitted for brevity. Note that, unlike for the exponential/Eyring model where solutions are possible for all values of $\hat{V}$, for the linear model solutions are possible only if $\hat{V}h_{\rm m} > -1$ in the limit $B \to 0$. In particular solutions for which $h_{\rm m} \to 1$ are possible only for $\hat{V} > -1$, while solutions for which $h_{\rm m} \to \infty$ are possible only for $\hat{V} \geq 0$.

The limit $\alpha \to 0$

In the limit $\alpha \to 0$ equation (47) again holds, but with the function $f(\hat{V})$ now given by (36) for $\hat{V} > -1$. The function $f(\hat{V})$ is plotted in Fig. 7 and satisfies

$$f = \frac{3}{2} - \frac{3}{2}(1+\hat{V}) + O((1+\hat{V})^2 \log(1+\hat{V})) \quad \text{as} \quad \hat{V} \to -1, \tag{A1}$$

$$f = 1 - \frac{\hat{V}}{4} + O(\hat{V}^2) \quad \text{as} \quad \hat{V} \to 0, \tag{A2}$$

$$f = \frac{3(2\log\hat{V} - 3)}{2\hat{V}} + O\left(\frac{\log\hat{V}}{\hat{V}^2}\right) \quad \text{as} \quad \hat{V} \to \infty. \tag{A3}$$

The limit $\alpha \to \pi$

In the limit $\alpha \to \pi$ the behaviour again depends on whether $\hat{V} > 0$, $\hat{V} = 0$ or $\hat{V} < 0$. Specifically, when $\hat{V} > 0$ we have

$$a \sim \pi - \left[\frac{3\pi(\pi-\alpha)}{2\bar{Q}\hat{V}}\mathrm{W}\left(\frac{\mathrm{e}^{-2/3}\bar{Q}\hat{V}^3}{6\pi(\pi-\alpha)}\right)\right]^{1/2} \sim \pi - \left[-\frac{3\pi(\pi-\alpha)}{2\bar{Q}\hat{V}}\log(\pi-\alpha)\right]^{1/2}, \tag{A4}$$

and

$$h_\mathrm{m} \sim \left[\frac{3\pi(\pi-\alpha)}{8\bar{Q}\hat{V}}\mathrm{W}\left(\frac{\mathrm{e}^{-2/3}\bar{Q}\hat{V}^3}{6\pi(\pi-\alpha)}\right)\right]^{-1/2} \sim \left[-\frac{3\pi(\pi-\alpha)}{8\bar{Q}\hat{V}}\log(\pi-\alpha)\right]^{-1/2} \to \infty, \tag{A5}$$

and when $\hat{V} = 0$ we recover the corresponding results in the isothermal case given by (52). There are no corresponding results when $\hat{V} < 0$, and so for the linear model the rivulet can run all the way to the bottom of the cylinder only when $\hat{V} \geq 0$.

The limit $\hat{V} \to \infty$

In the limit of strong cooling of the atmosphere $\hat{V} \to \infty$ the behaviour of the solution again depends on whether $0 \leq \alpha < \pi/2$, $\alpha = \pi/2$ or $\pi/2 < \alpha \leq \pi$. Specifically we have

$$a \sim \begin{cases} \dfrac{\bar{Q}\hat{V}m^2}{2\sin\alpha\log\hat{V}} \to \infty & \text{if} \quad 0 \leq \alpha < \pi/2, \\ \left[\dfrac{4}{45\bar{Q}\hat{V}}\mathrm{W}\left(90\mathrm{e}^{-46/5}\bar{Q}\hat{V}^4\right)\right]^{-1/3} \sim \left(\dfrac{45\bar{Q}\hat{V}}{16\log\hat{V}}\right)^{1/3} \to \infty & \text{if} \quad \alpha = \pi/2, \\ \dfrac{\pi}{m} - \dfrac{1}{m^2}\left[\dfrac{3\pi\sin\alpha}{2\bar{Q}\hat{V}m}\mathrm{W}\left(\dfrac{\mathrm{e}^{-2/3}\bar{Q}\hat{V}^3m}{6\pi\sin\alpha}\right)\right]^{1/2} \sim \dfrac{\pi}{m} - \dfrac{1}{m^2}\left(\dfrac{9\pi\sin\alpha\log\hat{V}}{2\bar{Q}\hat{V}m}\right)^{1/2} & \text{if} \quad \pi/2 < \alpha \leq \pi, \end{cases} \tag{A6}$$

and

$$h_\mathrm{m} \sim \begin{cases} \dfrac{1}{m} & \text{if} \quad 0 \leq \alpha < \pi/2, \\ \dfrac{1}{2}\left[\dfrac{4}{45\bar{Q}\hat{V}}\mathrm{W}\left(90\mathrm{e}^{-46/5}\bar{Q}\hat{V}^4\right)\right]^{-1/3} \sim \dfrac{1}{2}\left(\dfrac{45\bar{Q}\hat{V}}{16\log\hat{V}}\right)^{1/3} \to \infty & \text{if} \quad \alpha = \pi/2, \\ \left[\dfrac{3\pi\sin\alpha}{8\bar{Q}\hat{V}m}\mathrm{W}\left(\dfrac{\mathrm{e}^{-2/3}\bar{Q}\hat{V}^3m}{6\pi\sin\alpha}\right)\right]^{-1/2} \sim \left(\dfrac{8\bar{Q}\hat{V}m}{9\pi\sin\alpha\log\hat{V}}\right)^{1/2} \to \infty & \text{if} \quad \pi/2 < \alpha \leq \pi. \end{cases} \tag{A7}$$

Thus in $0 \leq \alpha < \pi/2$ we have $a = O(\hat{V}/\log\hat{V})$ and $h_{\rm m} = O(1)$, while in $\pi/2 < \alpha \leq \pi$ we have $a = O(1)$ and $h_{\rm m} = O(\hat{V}/\log\hat{V})^{1/2}$, and the adjustments between these two different types of asymptotic behaviour occur via boundary layers near $\alpha = \pi/2$ of thickness $O(\log\hat{V}/\hat{V})^{2/3}$.

The limit $\bar{Q} \to \infty$

In the limit of large flux $\bar{Q} \to \infty$ the behaviour of the solution again depends on whether $\hat{V} > 0$, $\hat{V} = 0$ or $\hat{V} < 0$ and on whether $0 \leq \alpha < \pi/2$, $\alpha = \pi/2$ or $\pi/2 < \alpha \leq \pi$. When $\hat{V} > 0$ we have

$$a \sim \begin{cases} \dfrac{3\bar{Q}m^3}{2f(\hat{V}/m)\sin\alpha} \to \infty & \text{if} \quad 0 \leq \alpha < \pi/2, \\ \left[\dfrac{4}{45\bar{Q}\hat{V}}\mathrm{W}\left(90\mathrm{e}^{-46/5}\bar{Q}\hat{V}^4\right)\right]^{-1/3} \sim \left(\dfrac{45\bar{Q}\hat{V}}{4\log\bar{Q}}\right)^{1/3} \to \infty & \text{if} \quad \alpha = \pi/2, \\ \dfrac{\pi}{m} - \dfrac{1}{m^2}\left[\dfrac{3\pi\sin\alpha}{2\bar{Q}\hat{V}m}\mathrm{W}\left(\dfrac{\mathrm{e}^{-2/3}\bar{Q}\hat{V}^3m}{6\pi\sin\alpha}\right)\right]^{1/2} \sim \dfrac{\pi}{m} - \dfrac{1}{m^2}\left(\dfrac{3\pi\sin\alpha\log\bar{Q}}{2\bar{Q}\hat{V}m}\right)^{1/2} & \text{if} \quad \pi/2 < \alpha \leq \pi, \end{cases} \tag{A8}$$

where the function $f(\hat{V}/m)$ is given by (36) and

$$h_{\rm m} \sim \begin{cases} \dfrac{1}{m} & \text{if} \quad 0 \leq \alpha < \pi/2, \\ \dfrac{1}{2}\left[\dfrac{4}{45\bar{Q}\hat{V}}\mathrm{W}\left(90\mathrm{e}^{-46/5}\bar{Q}\hat{V}^4\right)\right]^{-1/3} \sim \dfrac{1}{2}\left(\dfrac{45\bar{Q}\hat{V}}{4\log\bar{Q}}\right)^{1/3} \to \infty & \text{if} \quad \alpha = \pi/2, \\ \left[\dfrac{3\pi\sin\alpha}{8\bar{Q}\hat{V}m}\mathrm{W}\left(\dfrac{\mathrm{e}^{-2/3}\bar{Q}\hat{V}^3m}{6\pi\sin\alpha}\right)\right]^{-1/2} \sim \left(\dfrac{8\bar{Q}\hat{V}m}{3\pi\sin\alpha\log\bar{Q}}\right)^{1/2} \to \infty & \text{if} \quad \pi/2 < \alpha \leq \pi. \end{cases} \tag{A9}$$

When $\hat{V} = 0$ we recover the corresponding results in the isothermal case given by (78) and (79). When $\hat{V} < 0$ we have

$$a \sim \frac{3\bar{Q}m^3}{2f(\hat{V}/m)\sin\alpha} \to \infty, \quad h_{\rm m} \sim \frac{1}{m} \tag{A10}$$

for $0 \leq \alpha < \pi/2$, but there are no corresponding solutions for $\alpha = \pi/2$ and $\pi/2 < \alpha \leq \pi$. Thus, in $0 \leq \alpha < \pi/2$ we have $a = O(\bar{Q})$ and $h_{\rm m} = O(1)$ for all $\hat{V}$, while in $\pi/2 < \alpha \leq \pi$ we have $a = O(1)$ for all $\hat{V} \geq 0$ together with $h_{\rm m} = O(\bar{Q}/\log\bar{Q})^{1/2}$ when $\hat{V} > 0$ and $h_{\rm m} = O(\bar{Q}^{1/3})$ when $\hat{V} = 0$. The adjustments between these different types of asymptotic behaviour occur

via boundary layers near $\alpha = \pi/2$ of thickness $O(\log \bar{Q}/\bar{Q})^{2/3}$ when $\hat{V} > 0$ and $O(\bar{Q}^{-1/2})$ when $\hat{V} = 0$.

APPENDIX B: DETAILS OF THE ASYMPTOTIC ANALYSIS OF THE SOLUTION FOR THE EXPONENTIAL/EYRING MODEL IN THE LIMIT $\bar{Q} \to \infty$

In this appendix we give the details of the asymptotic analysis of the solution for the exponential/Eyring model in the limit $\bar{Q} \to \infty$ leading to the results given in Sec. III.G.

In the limit $\bar{Q} \to \infty$ the behaviour of the solution depends on whether $\hat{V} > 0$, $\hat{V} = 0$ or $\hat{V} < 0$ and on whether $0 \le \alpha < \pi/2$, $\alpha = \pi/2$ or $\pi/2 < \alpha \le \pi$. In each case once the asymptotic behaviour of a is known the corresponding behaviour of h_{m} can be calculated immediately from (20). The calculations in the case $\hat{V} = 0$ are omitted for brevity.

When $0 \le \alpha < \pi/2$ we have $a \to \infty$ and from (21) we have $h \sim 1/m$ (except in boundary layers near $y = \pm a$). Whatever the value of $\hat{V}$ from (32) we obtain $\bar{u} \sim f(\hat{V}/m)\sin\alpha/3m^3$; therefore from (34) we have $Q \sim 2af(\hat{V}/m)\sin\alpha/3m^3$, and so

$$a \sim \frac{3\bar{Q}m^3}{2f(\hat{V}/m)\sin\alpha} \to \infty. \tag{B1}$$

When $\alpha = \pi/2$ we have $a \to \infty$ and from (19) we have $h = (a^2 - y^2)/2a \to \infty$ (except in boundary layers near $y = \pm a$). When $\hat{V} > 0$ from (32) with (38) we obtain $\bar{u} \sim h^2/\hat{V}$; therefore from (34) we have

$$Q \sim \frac{1}{\hat{V}} \int_{-a}^{+a} \left(\frac{a^2 - y^2}{2a}\right)^2 \mathrm{d}y = \frac{4a^3}{15\hat{V}}, \tag{B2}$$

and so

$$a \sim \left(\frac{15\bar{Q}\hat{V}}{4}\right)^{1/3} \to \infty. \tag{B3}$$

When $\hat{V} < 0$ from (32) with (38) we obtain $\bar{u} \sim -2\exp(-\hat{V}h)/\hat{V}^3$; therefore from (34) we have

$$Q \sim -\frac{2}{\hat{V}^3} \int_{-\infty}^{+\infty} \exp\left(-\frac{\hat{V}(a^2 - y^2)}{2a}\right) \mathrm{d}y = \frac{4\sqrt{\pi}}{\hat{V}^4} \left(-\frac{\hat{V}a}{2}\right)^{1/2} \exp\left(-\frac{\hat{V}a}{2}\right), \tag{B4}$$

and so a satisfies

$$\left(-\frac{\hat{V}a}{2}\right)^{1/2}\exp\left(-\frac{\hat{V}a}{2}\right)\sim\frac{\bar{Q}\hat{V}^4}{4\sqrt{\pi}}, \tag{B5}$$

and hence

$$a\sim\frac{1}{(-\hat{V})}\mathrm{W}\left(\frac{\bar{Q}^2\hat{V}^8}{8\pi}\right)\sim\frac{2}{(-\hat{V})}\log\bar{Q}\to\infty, \tag{B6}$$

where we have used the fact that $\mathrm{W}(x)\sim\log x$ as $x\to\infty$. Equations (B3) and (B6) can also be obtained directly by using the appropriate asymptotic expansions given in section 2 of the exact expression for Q when $\alpha=\pi/2$ given in (40).

When $\pi/2<\alpha\leq\pi$ we have $a\to\pi/m^-$ and from (22) we have $h\sim(1+\cos my)/m(\pi-ma)\to\infty$ (except in boundary layers near $y=\pm a$). When $\hat{V}>0$ from (32) with (38) we obtain $\bar{u}\sim\sin\alpha\, h^2/\hat{V}$; therefore from (34) we have

$$Q\sim\frac{\sin\alpha}{\hat{V}}\int_{-\pi/m}^{+\pi/m}\left(\frac{1+\cos my}{m(\pi-ma)}\right)^2\mathrm{d}y\sim\frac{3\pi\sin\alpha}{\hat{V}m^3(\pi-ma)^2}, \tag{B7}$$

and so

$$a\sim\frac{\pi}{m}-\frac{1}{m^2}\left(\frac{3\pi\sin\alpha}{\bar{Q}\hat{V}m}\right)^{1/2}. \tag{B8}$$

When $\hat{V}<0$ from (32) with (38) we obtain $\bar{u}\sim-2\sin\alpha\exp(-\hat{V}h)/\hat{V}^3$; therefore from (34) we have

$$Q\sim-\frac{2\sin\alpha}{\hat{V}^3}\int_{-\pi/m}^{+\pi/m}\exp\left(-\frac{\hat{V}(1+\cos my)}{m(\pi-ma)}\right)\mathrm{d}y. \tag{B9}$$

Using Laplace's method (see, for example, Bender and Orszag [19]) gives

$$\int_{-\pi/m}^{+\pi/m}\exp\left(-\frac{\hat{V}(1+\cos my)}{m(\pi-ma)}\right)\mathrm{d}y\sim\frac{2\sqrt{\pi}}{m}\left(-\frac{2\hat{V}}{m(\pi-ma)}\right)^{-1/2}\exp\left(-\frac{2\hat{V}}{m(\pi-ma)}\right) \tag{B10}$$

and so a satisfies

$$\left(-\frac{2\hat{V}}{m(\pi-ma)}\right)^{-1/2}\exp\left(-\frac{2\hat{V}}{m(\pi-ma)}\right)\sim-\frac{\bar{Q}\hat{V}^3m}{4\sqrt{\pi}\sin\alpha}, \tag{B11}$$

and hence

$$a\sim\frac{\pi}{m}-\frac{4(-\hat{V})}{m^2}\left[-\mathrm{W}\left(-\frac{32\pi\sin^2\alpha}{\bar{Q}^2\hat{V}^6m^2}\right)\right]^{-1}\sim\frac{\pi}{m}-\frac{2(-\hat{V})}{m^2}\left(\log\bar{Q}\right)^{-1}, \tag{B12}$$

where we have used the fact that $\mathrm{W}(x)\sim\log(-x)$ as $x\to0^-$ on the relevant branch of W.

APPENDIX C: LAMBERT'S W FUNCTION

In this appendix we summarise the properties of Lambert's W function, $\mathrm{W} = \mathrm{W}(x)$, which is defined to be a solution of $\mathrm{W}\exp(\mathrm{W}) = x$. There are infinitely many complex branches of $\mathrm{W}(x)$, but for the present purpose we can restrict our attention to the real branches of $\mathrm{W}(x)$ shown in Fig. 9. These consist of a monotonically increasing branch defined on $[-1/\mathrm{e}, \infty)$ and satisfying $\mathrm{W}(-1/\mathrm{e}) = -1$, $\mathrm{W}(0) = 0$ and $\mathrm{W}(x) \sim \log x$ as $x \to \infty$, and a monotonically decreasing branch defined on $[-1/\mathrm{e}, 0)$ and satisfying $\mathrm{W}(-1/\mathrm{e}) = -1$ and $\mathrm{W}(x) \sim \log(-x)$ as $x \to 0^-$.

In deriving the asymptotic results presented in the present work we made use of the fact that for any $n \neq 0$ the solution of the algebraic equation $F^n \exp(F) = x$ can we written in terms of W as

$$F(x) = n\mathrm{W}\left(\frac{1}{n}x^{1/n}\right), \tag{C1}$$

and that the solution of the algebraic equation $G^n \log G = x$ can be written in terms of W as

$$G(x) = \exp\left(\frac{1}{n}\mathrm{W}(nx)\right) = \left(\frac{nx}{\mathrm{W}(nx)}\right)^{1/n}. \tag{C2}$$

References

[1] G. D. Towell and L. B. Rothfeld, "Hydrodynamics of rivulet flow," AIChE. J. **12**, 972–980 (1966).

[2] B. R. Duffy and H. K. Moffatt, "Flow of a viscous trickle on a slowly varying incline," Chem. Eng. J. **60**, 141–146 (1995).

[3] R. F. Allen and C. M. Biggin, "Longitudinal flow of a lenticular liquid filament down an inclined plane," Phys. Fluids **17**, 287–291 (1974).

[4] S. K. Wilson and B. R. Duffy, "On the gravity-driven draining of a rivulet of viscous fluid down a slowly varying substrate with variation transverse to the direction of flow," Phys. Fluids **10**, 13–22 (1998).

[5] S. K. Wilson, B. R. Duffy, and A. B. Ross, "On the gravity-driven draining of a rivulet of viscoplastic material down a slowly varying substrate," Phys. Fluids **14**, 555–571 (2002).

[6] P. C. Smith, "A similarity solution for slow viscous flow down an inclined plane," J. Fluid Mech. **58**, 275–288 (1973).

[7] B. R. Duffy and H. K. Moffatt, "A similarity solution for viscous source flow on a vertical plane," Euro. J. Appl. Math. **8**, 37–47 (1997).

[8] D. Holland, B. R. Duffy, and S. K. Wilson, "Thermocapillary effects on a thin viscous rivulet draining steadily down a uniformly heated or cooled slowly varying substrate," J. Fluid Mech. **441**, 195–221 (2001).

[9] S. K. Wilson and B. R. Duffy, "On the gravity-driven draining of a rivulet of fluid with temperature-dependent viscosity down a uniformly heated or cooled substrate," J. Eng. Maths **42**, 359–372 (2002).

[10] D. A. Goussis and R. E. Kelly, "Effects of viscosity variation on the stability of film flow down heated or cooled inclined surfaces: Long-wavelength analysis," Phys. Fluids **28**, 3207–3214 (1985).

[11] C.-C. Hwang and C.-I. Weng, "Non-linear stability analysis of film flow down a heated or cooled inclined plane with viscosity variation," Int. J. Heat Mass Transfer **31**, 1775–1784 (1988).

[12] B. Reisfeld and S. G. Bankoff, "Nonlinear stability of a heated thin liquid film with variable viscosity," Phys. Fluids A **2**, 2066–2067 (1990).

[13] M.-C. Wu and C.-C. Hwang, "Nonlinear theory of film rupture with viscosity variation," Int. Comm. Heat Mass Transfer **18**, 705–713 (1991).

[14] A. Oron, S. H. Davis, and S. G. Bankoff, "Long-scale evolution of thin liquid films," Rev. Mod. Phys **69**, 931–980 (1997).

[15] It is interesting to note that the specific choice of characteristic temperature scale is not so important in the corresponding problem when thermocapillary effects are significant (studied by Holland, Duffy and Wilson [8]) since, unlike in the present problem in which the viscosity varies by an $O(1)$ amount as T varies from T_0 to T_∞, in that problem the surface tension varies by only a (small) $O(\beta^2)$ amount as T varies from T_0 to T_∞, and so using the value of the surface tension at either $T = T_0$ or $T = T_\infty$ as the characteristic surface-tension scale is equally appropriate for both the experimental situation in which the temperature of the substrate is held fixed and that in which the temperature of the atmosphere is held fixed.

[16] In any particular physical experiment with $B \ll 1$ thermoviscosity effects are significant if $\hat{V} = O(1)$. Similarly, thermocapillary effects are significant if $M = O(1)$, where $M = \lambda_s \alpha_{th}(T_0 - T_\infty)/\rho g \beta l k_{th}$ is the effective Marangoni number used by Holland, Duffy and Wilson [8] in which $\lambda_s = -\mathrm{d}\gamma/\mathrm{d}T$ is a positive constant. Thus the present analysis (in which thermoviscosity effects are significant and thermocapillary effects are negligible) is applicable if $\hat{V} = O(1)$ and $M \ll 1$, and so, in particular, the condition $\mu_0 \lambda_s/\gamma\lambda \ll \beta^2 (\ll 1)$ must hold. For example, using the data for the variation of μ and γ with T for Bayer M-100 silicone oil and paraffin oil given by Ehrhard [17] shows that at 25 °C this condition holds when β is greater than approximately 20° for both fluids. Since the lubrication approximation typically remains accurate for relatively large values of β there

is a wide range of experimentally realisable values of β for which the present analysis applies.

[17] P. Ehrhard, "Experiments on isothermal and non-isothermal spreading," J. Fluid Mech. **257**, 463–483 (1993).

[18] Note that the functional dependencies of the fluidity f on $\hat{V}h$ for the linear and exponential/Erying models given by (36) and (38) coincide exactly with the functional dependencies of the fluidity f on $V = \hat{V}/B$ for the linear and exponential models in the limit $B \to \infty$ when $V = O(1)$ given by Wilson and Duffy [9, Eqns (36) and (39)].

[19] C. M. Bender and S. A. Orszag, *Advanced Mathematical Methods for Scientists and Engineers* (McGraw-Hill, 1978), pp. 265–276.

FIGURE CAPTIONS

FIG. 1 : The geometry of the problem.

FIG. 2 : The function $Q\hat{V}^4$ given by (39) for the linear model and by (40) for the exponential/Eyring model plotted as functions of $\hat{V}a$. Note that for both models $Q\hat{V}^4$ satisfies $Q\hat{V}^4 = 4(\hat{V}a)^4/105 - 4(\hat{V}a)^5/945 + O(\hat{V}a)^6$ as $\hat{V}a \to 0$, and that for the linear model $Q\hat{V}^4$ is defined only for $\hat{V}a > -2$.

FIG. 3 : Sketch of a slowly varying rivulet draining in the azimuthal direction from the top ($\alpha = 0$) to the bottom ($\alpha = \pi$) of a large horizontal circular cylinder.

FIG. 4 : (a) The semi-width of the rivulet a, and (b) the maximum thickness of the rivulet $h_{\rm m}$ plotted as functions of α/π for a range of values of $\hat{V}$ in the case $\bar{Q} = 1$. The leading-order asymptotic values in the limit $\hat{V} \to \infty$ given by $a \sim \pi/|\cos\alpha|^{1/2}$ for $\pi/2 < \alpha \leq \pi$ and by $h_{\rm m} \sim 1/(\cos\alpha)^{1/2}$ for $0 \leq \alpha < \pi/2$ are marked with dashed lines.

FIG. 5 : (a) The semi-width of the rivulet a, and (b) the maximum thickness of the rivulet $h_{\rm m}$ plotted as functions of α/π for a range of values of $\bar{Q}$ in the case $\hat{V} = 1$. The leading-order asymptotic values in the limit $\bar{Q} \to \infty$ given by $a \sim \pi/|\cos\alpha|^{1/2}$ for $\pi/2 < \alpha \leq \pi$ and by $h_{\rm m} \sim 1/(\cos\alpha)^{1/2}$ for $0 \leq \alpha < \pi/2$ are marked with dashed lines.

FIG. 6 : As for Fig. 4 except that $\hat{V} = -1$.

FIG. 7 : The functions $f(\hat{V})$ given by (36) for the linear model and by (38) for the exponential/Eyring model plotted as functions of $\hat{V}$. Note that for both models $f(\hat{V})$ satisfies $f = 1 - \hat{V}/4 + O(\hat{V}^2)$ as $\hat{V} \to 0$, and that for the linear model $f(\hat{V})$ is defined only for $\hat{V} > -1$.

FIG. 8 : (a) a_1 and (b) h_{m1}, the first-order corrections to the semi-width and the height of the rivulet respectively in the limit of weak cooling or heating $\hat{V} \to 0$, plotted as functions of α/π in the case $\bar{Q} = 1$.

FIG. 9 : The real branches of Lambert's W function, $\mathrm{W} = \mathrm{W}(x)$.

Figure 1, Wilson and Duffy, *Phys. Fluids*

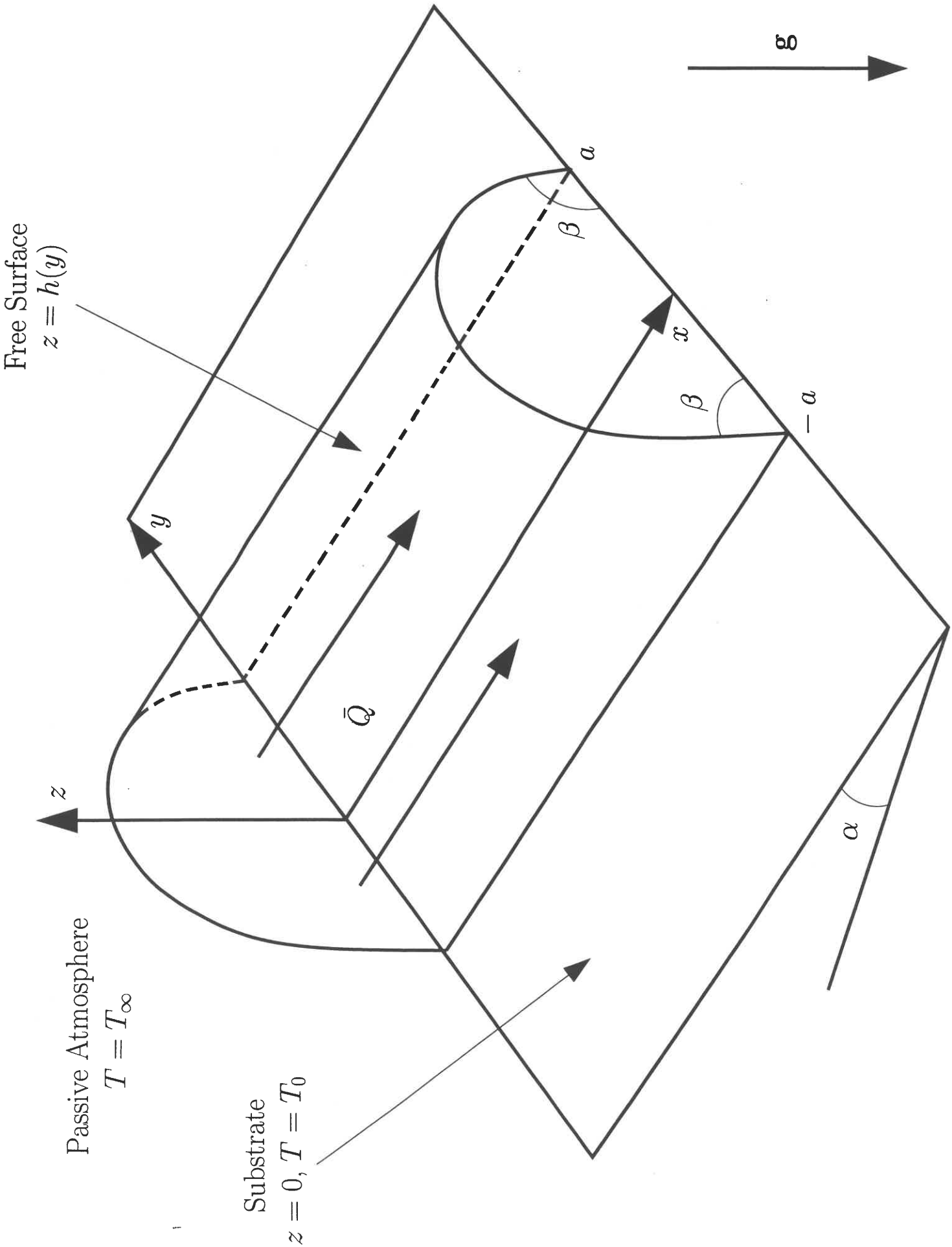

Figure 2, Wilson and Duffy, *Phys. Fluids*

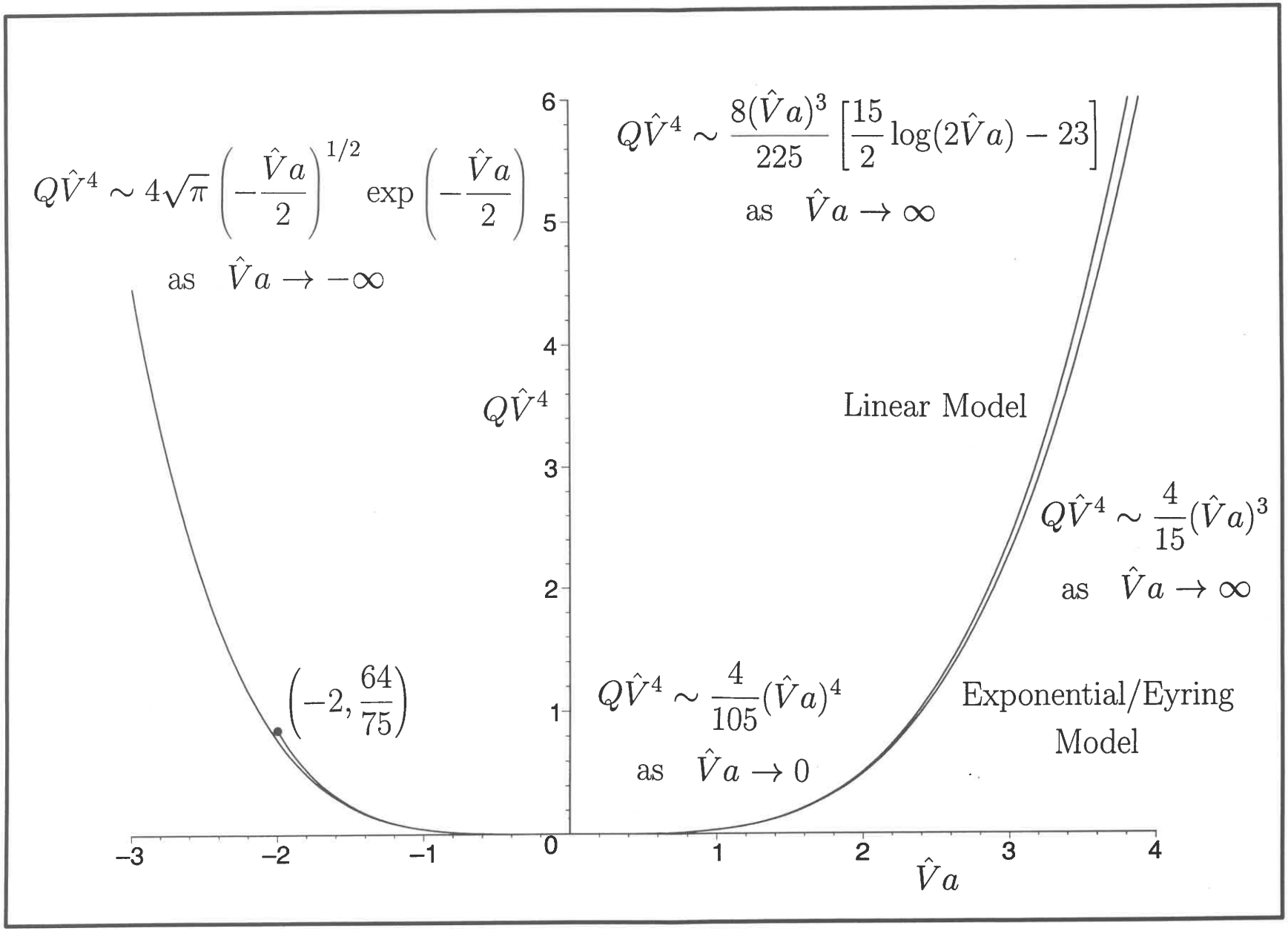

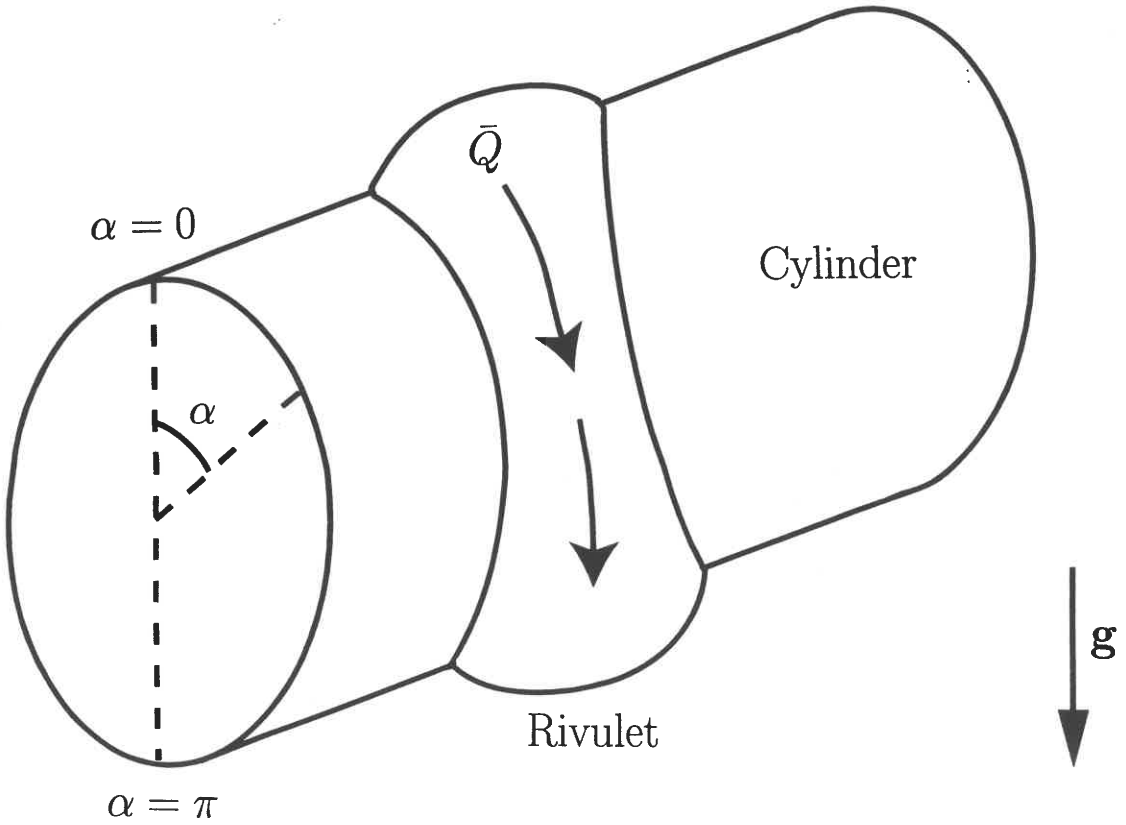

Figure 3, Wilson and Duffy, *Phys. Fluids*

Figure 4(a), Wilson and Duffy, *Phys. Fluids*

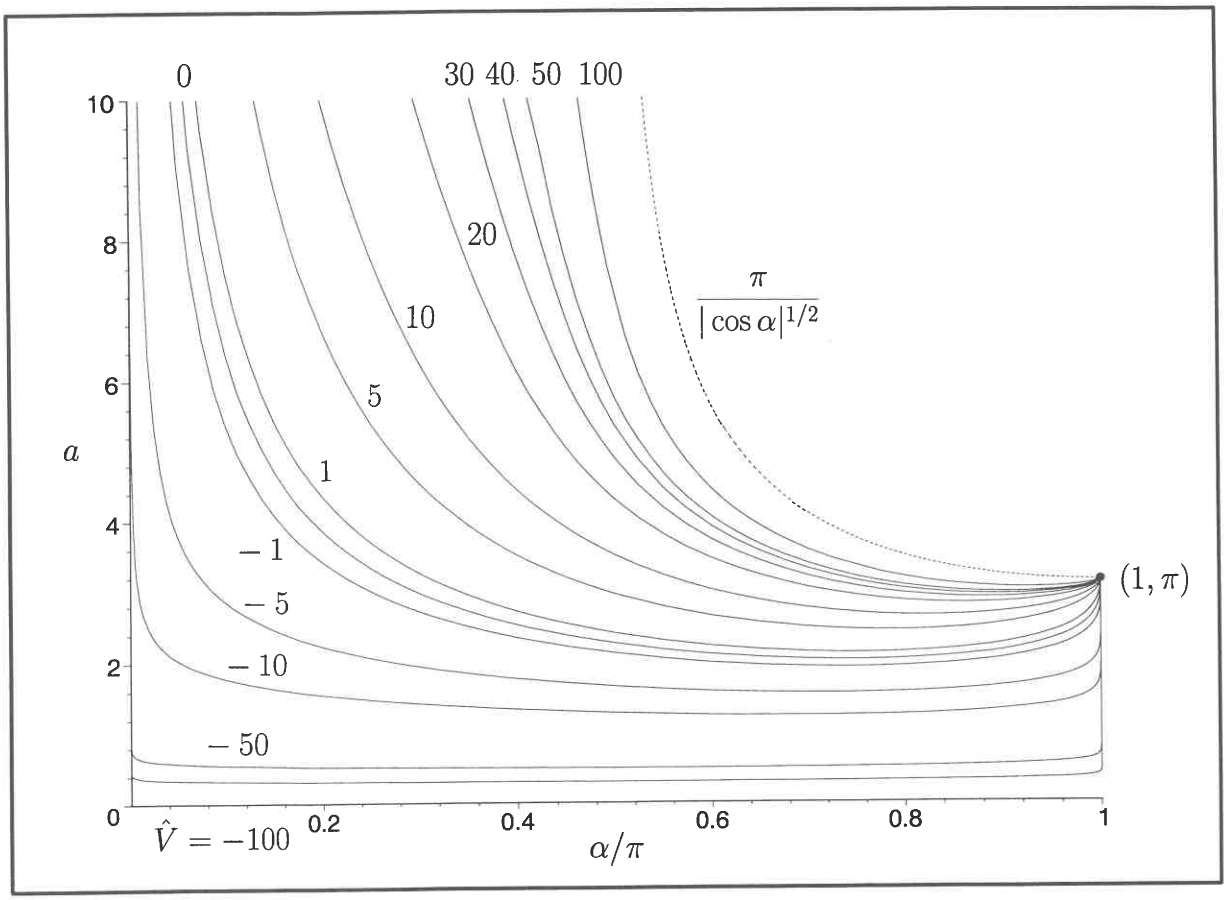

Figure 4(b), Wilson and Duffy, *Phys. Fluids*

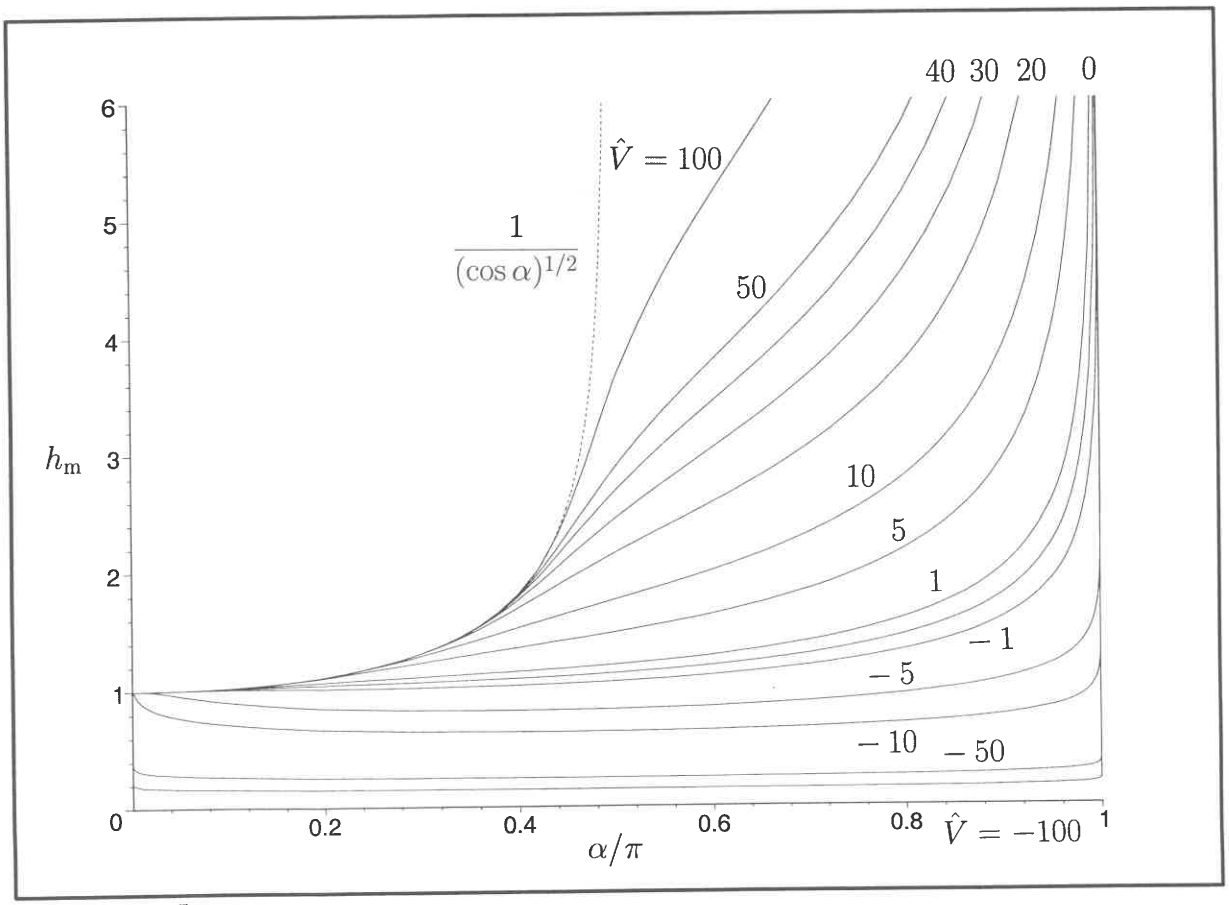

Figure 5(a), Wilson and Duffy, *Phys. Fluids*

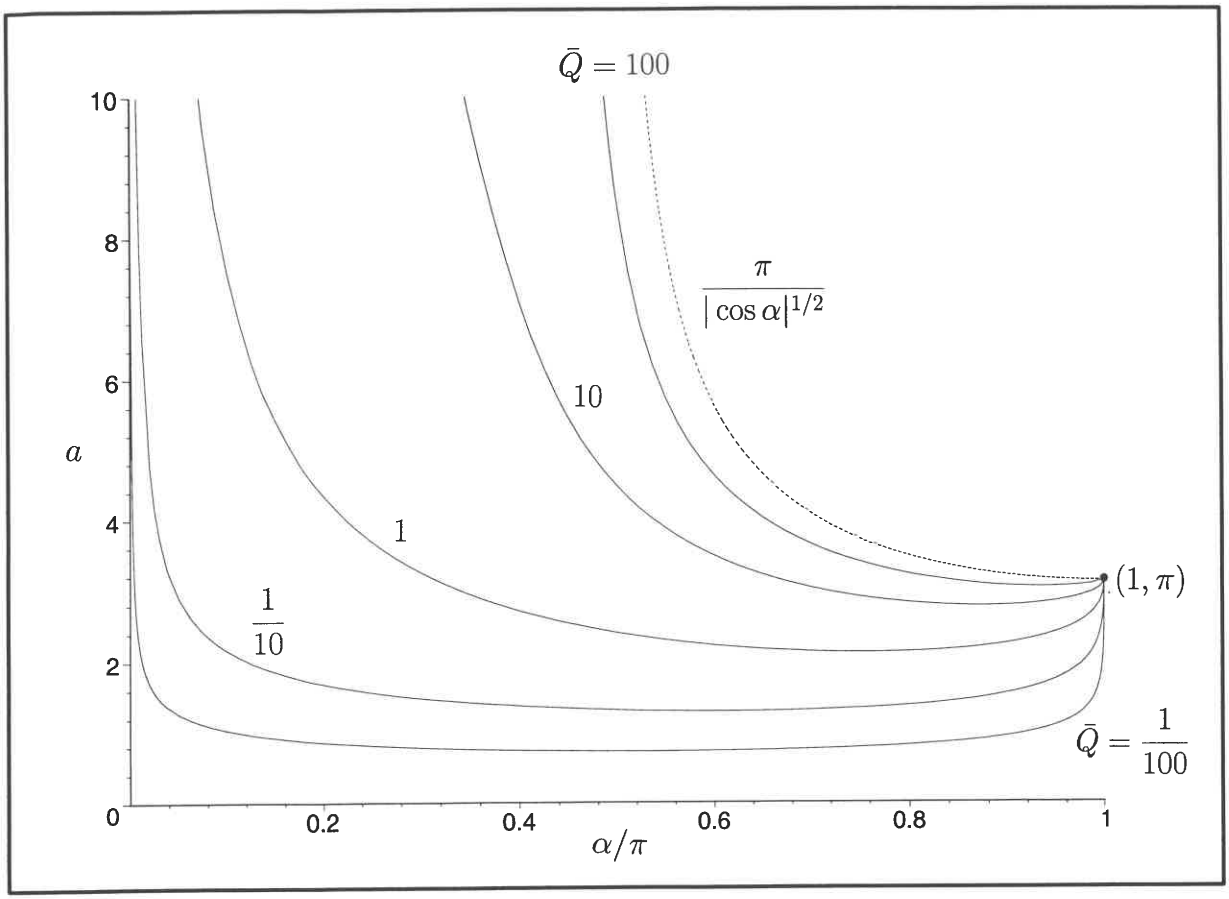

Figure 5(b), Wilson and Duffy, *Phys. Fluids*

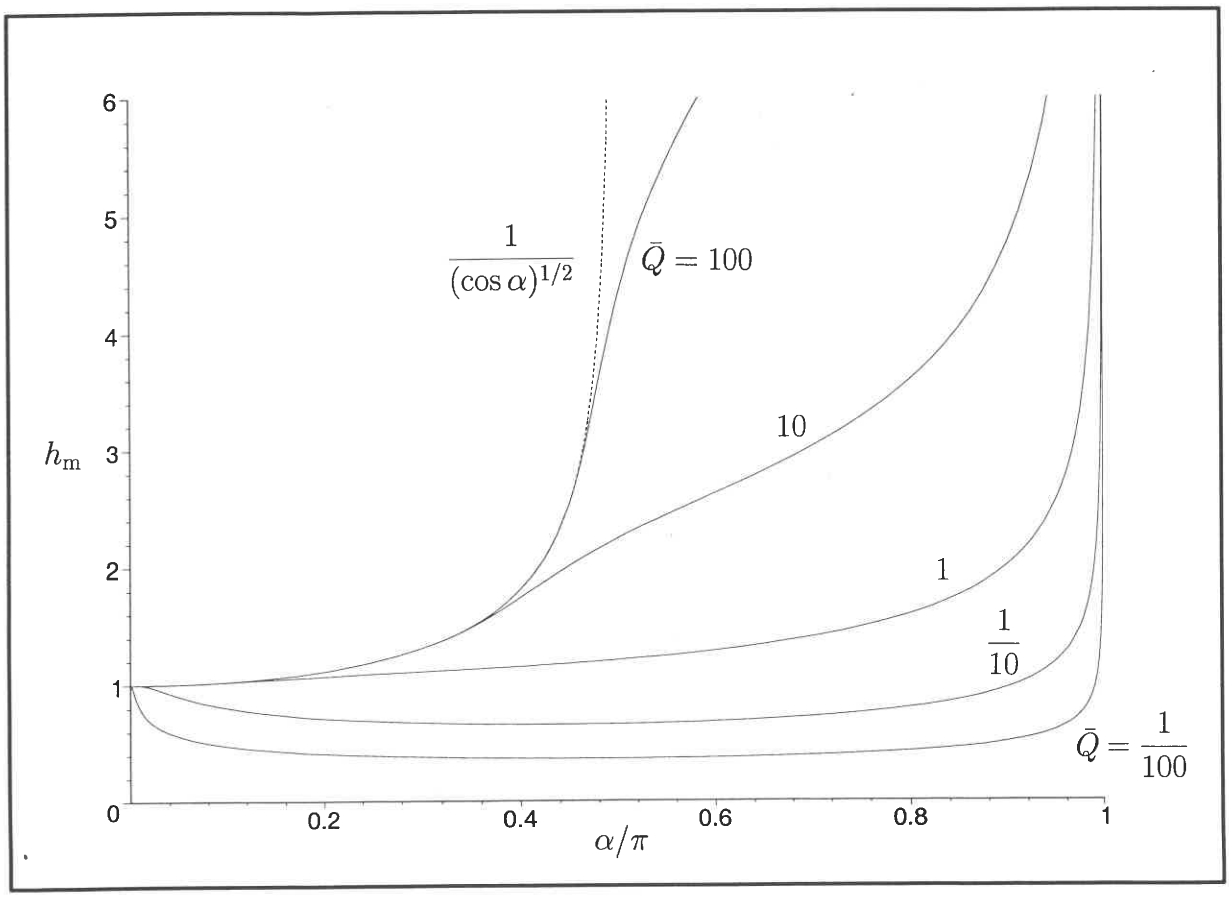

Figure 6(a), Wilson and Duffy, *Phys. Fluids*

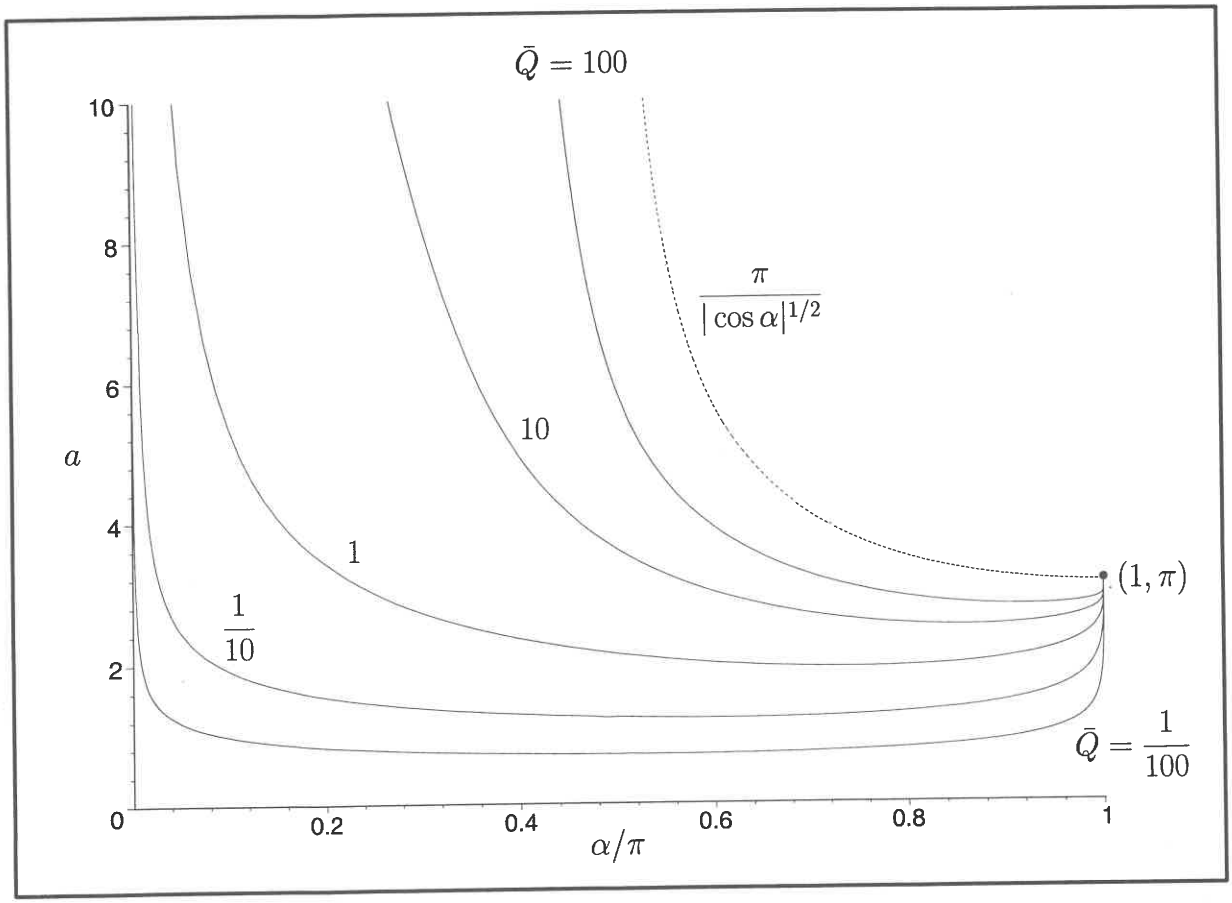

Figure 6(b), Wilson and Duffy, *Phys. Fluids*

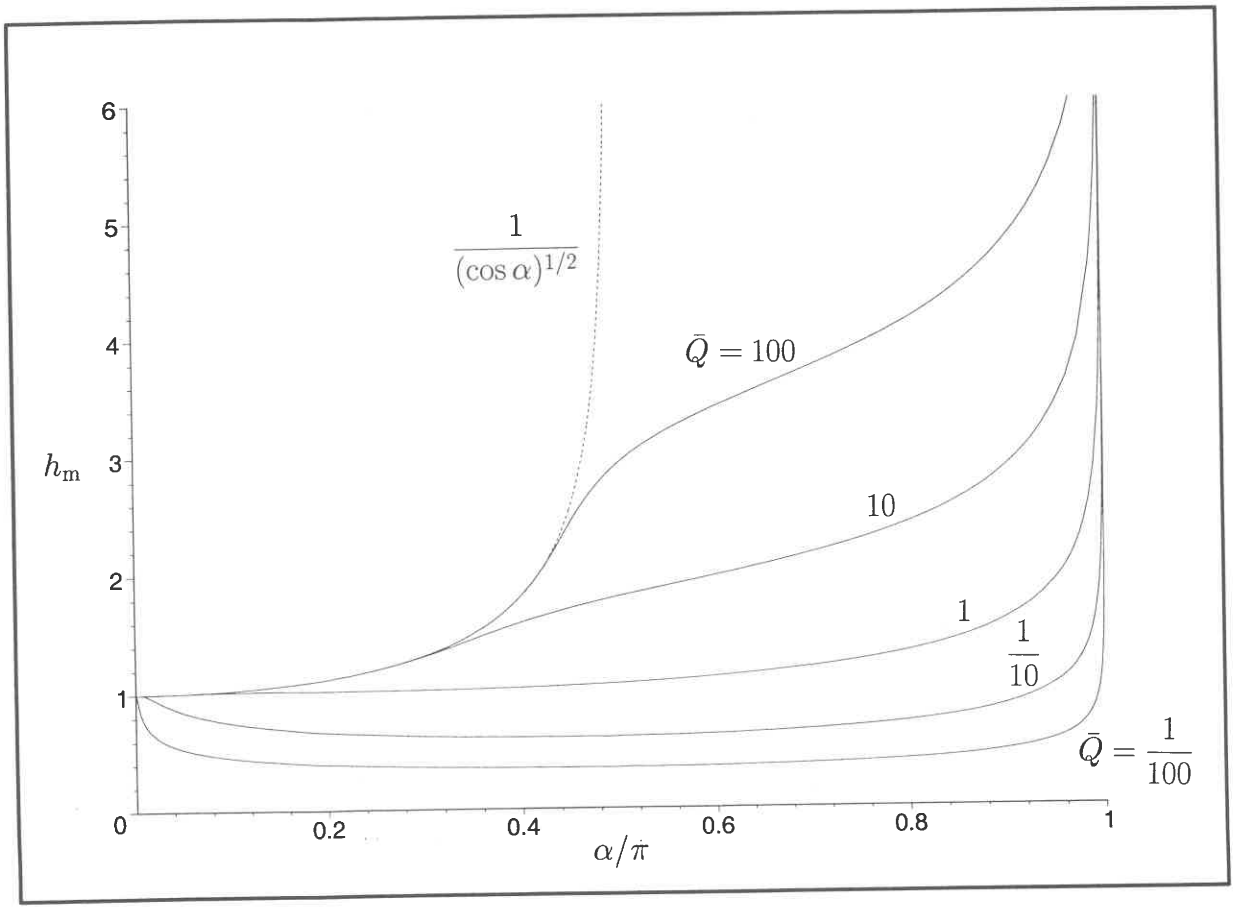

Figure 7, Wilson and Duffy, *Phys. Fluids*

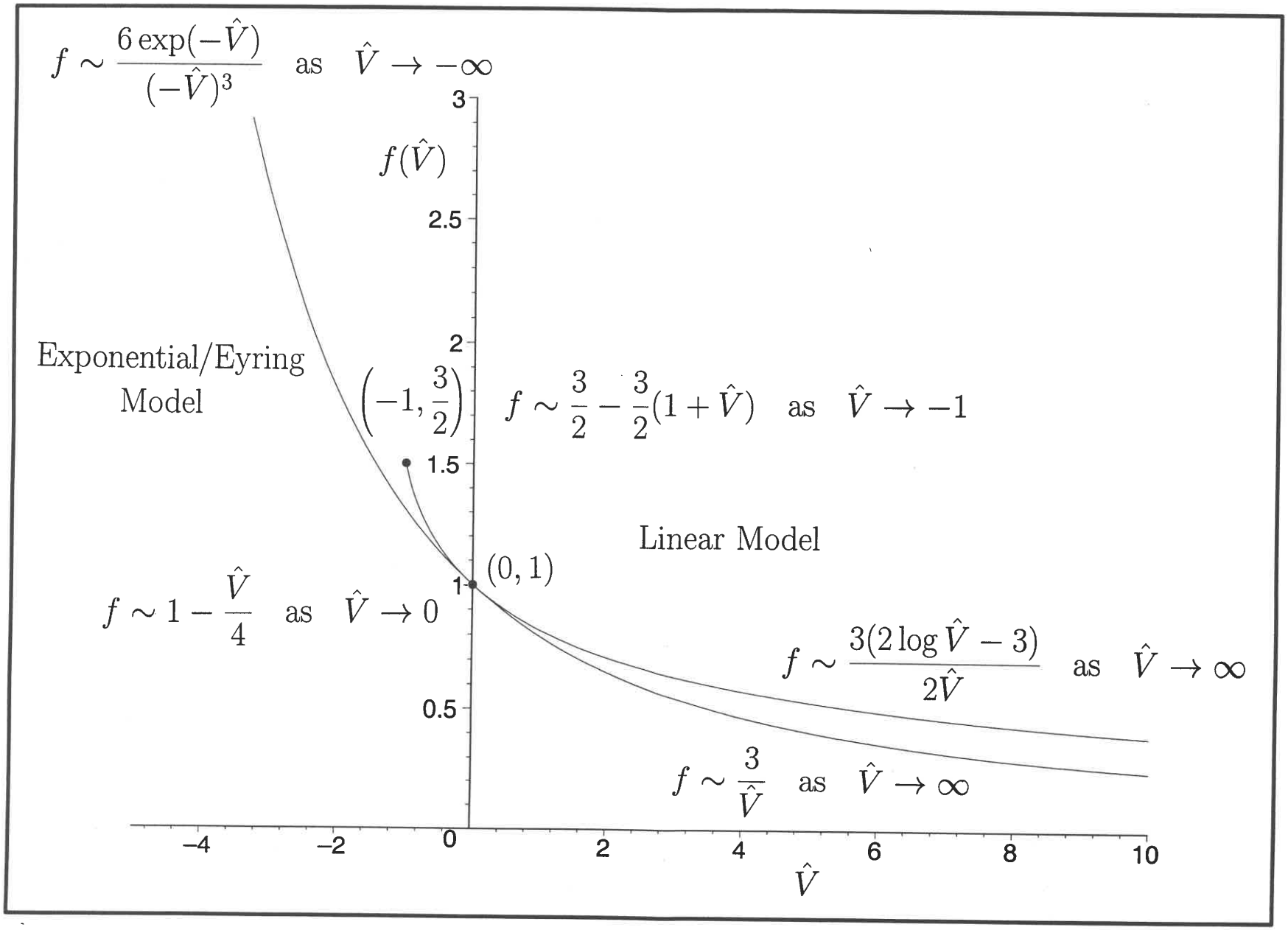

Figure 8, Wilson and Duffy, *Phys. Fluids*

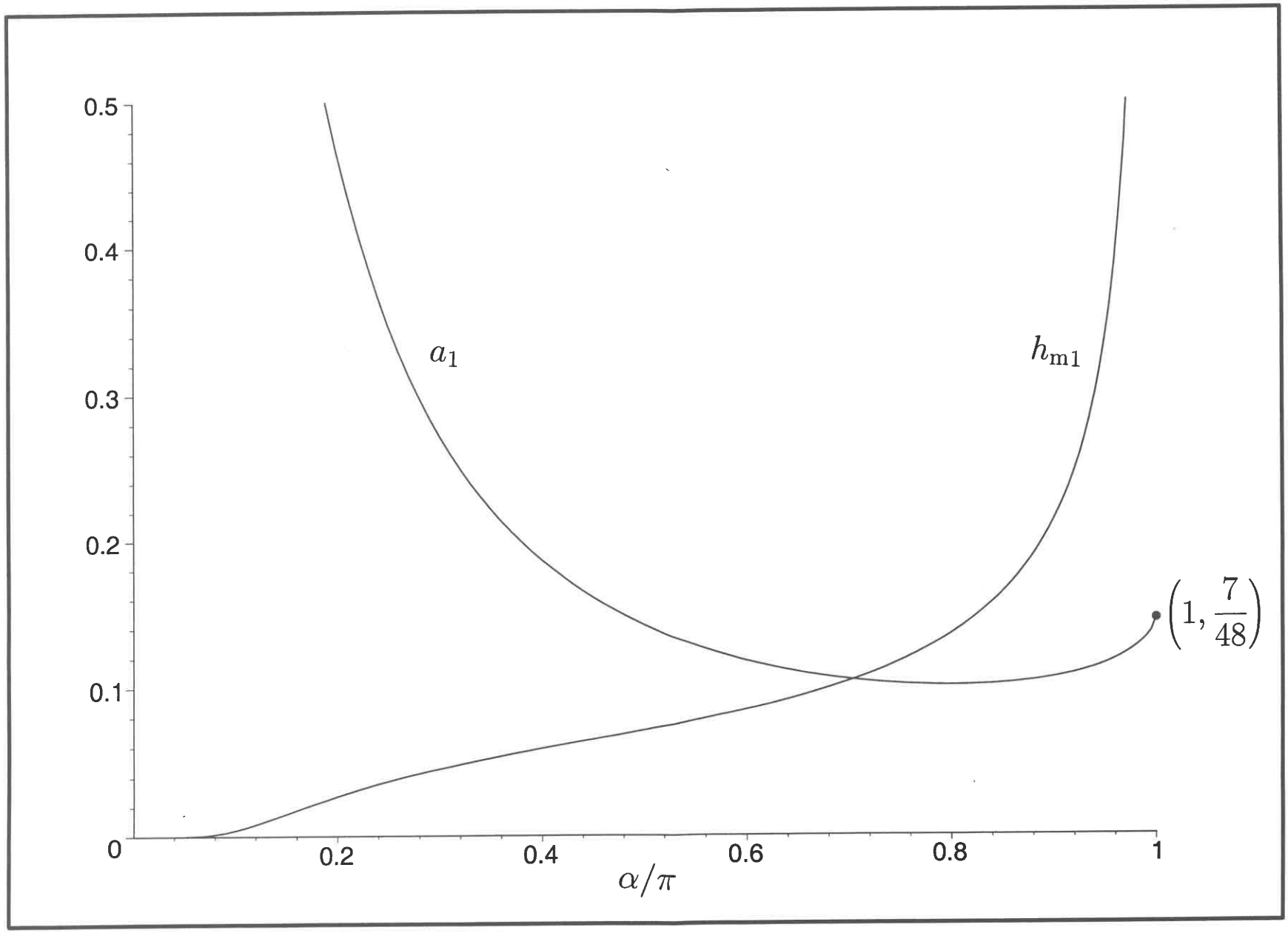

Figure 9, Wilson and Duffy, *Phys. Fluids*